

# Quantum optics of ultra-cold molecules

D. Meiser, T. Miyakawa, H. Uys, and P. Meystre

*Department of Physics, The University of Arizona, 1118 E. 4th Street, Tucson, Arizona, 85705*

Quantum optics has been a major driving force behind the rapid experimental developments that have led from the first laser cooling schemes to the Bose-Einstein condensation (BEC) of dilute atomic and molecular gases. Not only has it provided experimentalists with the necessary tools to create ultra-cold atomic systems, but it has also provided theorists with a formalism and framework to describe them: many effects now being studied in quantum-degenerate atomic and molecular systems find a very natural explanation in a quantum optics picture. This article briefly reviews three such examples that find their direct inspiration in the trailblazing work carried out over the years by Herbert Walther, one of the true giants of that field. Specifically, we use an analogy with the micromaser to analyze ultra-cold molecules in a double-well potential; study the formation and dissociation dynamics of molecules using the passage time statistics familiar from superradiance and superfluorescence studies; and show how molecules can be used to probe higher-order correlations in ultra-cold atomic gases, in particular bunching and antibunching.

## I. INTRODUCTION

Quantum optics plays a central role in the physics of quantum-degenerate atoms and molecules. Laser light and its coherent and incoherent interactions with atoms are ubiquitous in these experiments, and the tools that have culminated in the achievement of Bose-Einstein condensation (BEC) (Anderson et al., 1995; Bradley et al., 1995; Davis et al., 1995) were first studied and understood in quantum optics. Indeed, the deep connection between quantum optics and cold atom physics was realized well before the first experimental realizations of BEC, both at the experimental and theoretical levels. On the theory side, there are (at least) two important reasons why quantum optics methods are well suited for the study of cold atoms systems. First, bosonic fields have direct analogs in electromagnetic fields, which have been extensively studied in quantum optics. Second, for fermions the Pauli Exclusion Principle restricts the occupation of a given mode to zero or one, and these two states — mode occupied or empty — can often be mapped onto a two-level system, as we shall see. As a result, many situations familiar from quantum optics are also found in cold-atom systems, including matter-wave interference (Andrews et al., 1997), atom lasers and matter-wave amplifiers (Inouye et al., 1999b; Ketterle and H.-J. Miesner, 1997; Kozuma et al., 1999; Law and Bigelow, 1998), matter-wave beam splitters (Burgbacher and Audretsch, 1999), four-wave mixing (Christ et al., 2003; Lenz et al.,

1993; Meiser et al., 2005a; Miyakawa et al., 2003; Moore et al., 1999; Rojo et al., 1999; Search et al., 2002b), and Dicke superradiance (Inouye et al., 1999a; Moore and Meystre, 1999), to name a few.

At the same time the physics of ultra-cold atoms is much richer than its quantum-optical counterpart since atoms can be either fermions (DeMarco and Jin, 1998, 1999; Hadzibabic et al., 2003) or bosons and have a rich internal structure. In addition, the interaction between atoms can be tuned relatively easily on fast time scales using for instance Feshbach resonances (Duine and Stoof, 2004; Dürr et al., 2004; Inouye et al., 1998, 2004; Stan et al., 2004; Timmermans et al., 1999) or two-photon Raman transitions (Theis et al., 2004; Wynar et al., 2000). Indeed, some of the most exciting recent developments in the physics of ultra-cold atoms are related to the coherent coupling of atoms to ultra-cold molecules by means of Feshbach resonances (Dürr et al., 2004; Regal et al., 2003), and photo-association (Kerman et al., 2004; Wynar et al., 2000). Both bosons and fermions have been successfully converted into molecules. In both cases BEC of molecules has been observed (Donley et al., 2002; Greiner et al., 2003; Jochim et al., 2003; Zwierlein et al., 2003), and the long-standing question of the BEC-BCS crossover is being investigated experimentally and theoretically in those systems (Bartenstein et al., 2004; Holland et al., 2001; Ohashi and Griffin, 2002; Regal et al., 2004a; Timmermans et al., 2001; Zwierlein et al., 2004). Other developments with close connections with quantum optics include the trapping of atoms in optical lattices (Greiner et al., 2002a,b; Jaksch et al., 1998), which play a role closely related to a high-Q resonator in cavity QED (Search et al., 2004; Walther, 1992) and leads in addition to fascinating connections with condensed matter physics and quantum information science.

With so many close connections between the physics of quantum-degenerate atomic and molecular systems and quantum optics, it is natural and wise to go back to the masters of that field to find inspiration and guidance, and this is why Herbert Walther's intellectual imprint remains so important. This brief review illustrates this point with three examples. Section II shows that the conversion of pairs of fermions into molecules in a double-well potential can be described by a generalized Jaynes-Cummings model. Using this equivalence, we show that the dynamics of the molecular field at each site can be mapped to that of a micromaser, one of Herbert Walther's most remarkable contributions (Meschede et al., 1985). Section III further expands on the mapping of ultra-cold fermion pairs onto two-level atoms to study the role of fluctuations in the association and dissociation rates of ultra-cold molecules. We show that this system is closely related to Dicke superradiance, and with this analogy as a guide, we discuss how the passage time fluctuations depend sensitively on the initial state of the system. In a third example, inspired by Herbert Walther's work on photon statistics and antibunching (Brattke et al., 2001; Krause et al., 1989; Rempe et al., 1990; Rempe and Walther, 1990) section IV analyzes how the statistics of their constituent atoms affects

the counting statistics of molecules formed by photo-association. We compare the three cases where the molecules are formed from a BEC, an ultra-cold Fermi gas and a Fermi system with a superfluid component. The concept of quantum coherence developed by R. J. Glauber and exploited in many situations by H. Walther and his coworkers, in particular in their studies of resonance fluorescence, are now applied to characterizing the statistical properties of the coupled atom-molecule system. Finally, section V further elaborates on these ideas to probe spatial correlations and coherent properties of atomic samples, and we find that the momentum distribution of the molecules contains detailed information about the second-order correlations of the initial atomic gas.

## II. MOLECULAR MICROMASER

Ultra-cold atoms and molecules trapped in optical lattices provide an exciting new tool to study a variety of physics problems. In particular, they provide remarkable connections with the condensed matter of strongly correlated systems and with quantum information science, a very well controlled environment to study processes such as photo-association (Ryu et al., 2005), and, from a point-of-view more directly related to quantum optics, can be thought of as matter-wave analog of photons trapped in high- $Q$  cavities. In particular, the high degree of real-time control of the system parameters offers the opportunity to directly experimentally study some of the long-standing questions of condensed matter physics, such as the ground state structure of certain models and many-body dynamic properties (Jaksch and Zoller, 2005). The coherent formation of molecules in an optical lattice via either Feshbach resonances and two-photon Raman photo-association has been studied both theoretically (Damski et al., 2003; Esslinger and Molmer, 2003; Jaksch et al., 2002; Molmer, 2003; Moore and Sadeghpour, 2003) and experimentally (Kohl et al., 2005; Rom et al., 2004; Ryu et al., 2005; Stoferle et al., 2005). In particular, the experiment of Ref. (Ryu et al., 2005) observed reversible and coherent Rabi oscillations in a gas of coupled atoms and molecules.

The idea of the molecular micromaser (Search et al., 2003) relies on the observation that, as a consequence of Fermi statistics, the photo-association of fermionic atoms into bosonic molecules can be mapped onto a generalized Jaynes-Cummings model. This analogy allows one to immediately translate many of the results that have been obtained for the Jaynes-Cummings model to atom-molecule systems. In addition, the molecular system possesses several properties that have no counterpart in the quantum optics analog, giving rise to interesting generalizations of the original micromaser problem (Filipowicz et al., 1986; Guzman et al., 1989; Meschede et al., 1985; Remoe et al., 1990). One of these new features is the inter-site tunneling of atoms and molecules between adjacent lattice sites, leading to a system that can be thought of as an array of molecular micromasers (Search et al., 2004).

To see how this works, rather than treating a full lattice potential we consider the dynamics of the molecular field in the simpler model of a coupled atom-molecule system in a double-well potential. We first show that inter-well tunneling enhances number fluctuations and eliminates trapping states in a manner similar to thermal fluctuations. We also examine the buildup of the relative phase between the two molecular states localized at the two wells due to the combined effect of inter-well tunneling and two-body collisions. We identify three regimes, characterized by different orders of magnitude of the ratio of the two-body collision strength to the inter-well tunneling coupling. The crossover of the non-equilibrium steady state from a phase-coherent regime to a phase-incoherent regime is closely related to the phase locking of condensates in Josephson-type configurations (Leggett, 2001), while we consider an open quantum system with incoherent pump and molecular loss which results in a dissipative steady state.

### A. Model

We consider a mixture of two hyperfine spin states  $|\sigma = \uparrow, \downarrow\rangle$  of fermionic atoms of mass  $m_f$  trapped in a double-well potential at temperature  $T = 0$ , which can be coherently combined into bosonic molecules of mass  $m_b$  via two-photon Raman photo-association. If the band-gap of the lattice potential is much larger than any other energy scale in the system, the fermions and molecules occupy only the lowest energy level of each well and the number of fermions of a given spin state is at most one in each well.

In the tight binding approximation, the effective Hamiltonian describing the coupled atom-molecule system is

$$\hat{H} = \sum_{i=l,r} (\hat{H}_{0i} + \hat{H}_{Ii}) + \hat{H}_T, \quad (1)$$

where

$$\begin{aligned} \hat{H}_{0i} = & \hbar(\omega_b + \delta)\hat{n}_i + \hbar\omega_f(\hat{n}_{\uparrow i} + \hat{n}_{\downarrow i}) + \frac{1}{2}\hbar U_b \hat{n}_i(\hat{n}_i - 1) \\ & + \hbar U_x \hat{n}_i(\hat{n}_{\uparrow i} + \hat{n}_{\downarrow i}) + \hbar U_f \hat{n}_{\uparrow i} \hat{n}_{\downarrow i}, \end{aligned} \quad (2)$$

$$\hat{H}_{Ii} = \hbar\chi(t)\hat{b}_i^\dagger \hat{c}_{\uparrow i} \hat{c}_{\downarrow i} + H.c., \quad (3)$$

$$\hat{H}_T = -\hbar J_b \hat{b}_l^\dagger \hat{b}_r - \hbar J_f (\hat{c}_{\uparrow l}^\dagger \hat{c}_{\uparrow r} + \hat{c}_{\downarrow l}^\dagger \hat{c}_{\downarrow r}) + H.c. \quad (4)$$

Here  $\hat{c}_{\sigma i}$  and  $\hat{b}_i$ ,  $i = l, r$ , are the annihilation operators of fermionic atoms and bosonic molecules in the left ( $l$ ) and right ( $r$ ) wells, respectively. The corresponding number operators  $\hat{n}_i = \hat{b}_i^\dagger \hat{b}_i$  and  $\hat{n}_{\sigma i} = \hat{c}_{\sigma i}^\dagger \hat{c}_{\sigma i}$  have eigenvalues  $n_i$  and  $n_{\sigma i}$ , respectively, and  $\hbar\omega_b$  and  $\hbar\omega_f$  are the energies of the molecules and atoms in the isolated wells.

The terms proportional to  $U_b$ ,  $U_x$ , and  $U_f$  in  $\hat{H}_{0i}$  describe on-site two-body interactions between molecules, between atoms and molecules, and between atoms, respectively. The interaction Hamiltonian  $\hat{H}_{Ii}$  describes the con-

version of atoms into molecules via two-photon Raman photo-association. The photo-association coupling constant  $\chi(t)$  is proportional to the far off-resonant two-photon Rabi frequency associated with two nearly co-propagating lasers (Heinzen et al., 2000), and  $\delta$  is the two-photon detuning between the lasers and the energy difference of the atom pairs and the molecules. The tunneling between two wells is described by the parameters  $J_b$  and  $J_f$  in the tunneling Hamiltonian  $\hat{H}_T$ .

The molecular field is “pumped” by a train of short photo-association pulses of duration  $\tau$ , separated by long intervals  $T \gg \tau$  during which the molecules are subject only to two-body collisions and quantum tunneling between the potential wells, as well as to losses due mainly to three-body collisions and collisional relaxation to low-lying vibrational states. In the absence of inter-well tunneling, this separation of time scales leads to a situation very similar to that encountered in the description of traditional micromasers, with the transit of individual two-level atoms through the micromaser cavity replaced by the train of photo-association pulses.

The dynamics of the molecular field in the double-well system is governed by the following four mechanisms:

(i) Coherent pumping by injection of pairs of fermionic atoms inside the double-well. This process is the analog of the injection of two-level atoms into a micromaser cavity. The injection of pairs of fermionic atoms into the double-well potential can be accomplished e.g. by Raman transfer of atoms from an untrapped internal state (Jaksch et al., 1998; Mandel et al., 2004). This results in the pumping of fermions into the double well at a rate  $\Gamma$  (Search et al., 2002a). We assume that for times  $T \gg \Gamma^{-1}$ , a pair of fermions has been transferred to the two wells with unit probability, that is, the state of the trapped fermions in well  $i$  is

$$|e_i\rangle = \hat{c}_{\downarrow i}^\dagger \hat{c}_{\uparrow i}^\dagger |0\rangle. \quad (5)$$

(ii) Molecular damping, which is the analog of cavity damping. During the time intervals  $T$  when the photo-association lasers are off, the molecular field decays at rate  $\gamma$  (Search et al., 2003). The decay of the molecules is due to Rayleigh scattering from the intermediate molecular excited state, three-body inelastic collisions between a molecule and two fermions, and collisional relaxation from a vibrationally excited molecular state to deeply bound states. These loss mechanisms can be modeled by a master equation, see e.g. (Meystre and III, 1999; Miyakawa et al., 2004; Scully and Zubairy, 1997).

(iii) The application of a train of photo-association pulses. This mechanism is formally analogous to the Jaynes-Cummings interaction between the single-mode field and a sequence of two-level atoms traveling through the microwave cavity in the conventional micromaser. As already mentioned, we assume that these are square pulses of duration  $\tau$  and period  $T + \tau$ , with  $\tau$  much shorter than all other time scales in this model,  $\tau \ll J_{b,f}^{-1}, \gamma^{-1}$ . This assumption

is essential if we are to neglect damping and tunneling while the photo-association fields are on. The change in the molecular field resulting from atom-molecule conversion is given by

$$F_i(\tau)\hat{\rho}_b \equiv Tr_a[U_i(\tau)\hat{\rho}_{ab}(t)U_i^\dagger(\tau)], \quad (6)$$

where  $\hat{\rho}_{ab}$  is the total density operator of the atom-molecule system and  $Tr_a[ \ ]$  denotes the trace over the atomic variables,  $U_i(\tau) = \exp(-i\hat{h}_i\tau/\hbar)$  being the evolution operator for a single-well Hamiltonian,

$$\hat{h}_i = \hat{H}_{0i} + \hat{H}_{Ii}.$$

The key observation that allows us here and below to build a bridge from the cold atoms and molecular system to quantum optics systems is that by means of the mapping (Anderson, 1958)

$$\begin{aligned} \hat{\sigma}_{-i} &= c_{\uparrow i}c_{\downarrow i}, \\ \hat{\sigma}_{+i} &= c_{\downarrow i}^\dagger c_{\uparrow i}^\dagger, \\ \hat{\sigma}_{zi} &= c_{\uparrow i}^\dagger c_{\uparrow i} + c_{\downarrow i}^\dagger c_{\downarrow i} - 1, \end{aligned} \quad (7)$$

the atomic degrees of freedom take the form of a fictitious two level system. The operators  $\hat{\sigma}_{+i}, \hat{\sigma}_{-i}$ , and  $\hat{\sigma}_{zi}$  can be interpreted as the raising and lowering operators of the fictitious two-level atom and the population difference, respectively. The single-well Hamiltonian takes the form

$$\begin{aligned} \hat{h}_i &= \hbar(\omega_b + U_x)\hat{n}_i + \hbar(\omega_f + U_x\hat{n}_i)\hat{\sigma}_{zi} \\ &+ \hbar\left(\chi(t)\hat{b}_i^\dagger\hat{\sigma}_{-i} + \chi^*(t)\hat{b}_i\hat{\sigma}_{+i}\right) + \frac{\hbar}{2}U_b\hat{n}_i(\hat{n}_i - 1) \end{aligned} \quad (8)$$

where we have dropped constant terms and we have redefined  $\omega_b + \delta \rightarrow \omega_b$  and  $\omega_f + U_f/2 \rightarrow \omega_f$ .

The Hamiltonian  $\hat{h}_i$  is Jaynes-Cummings-like, and for  $\chi = \text{const.}$ , the resulting dynamics can be determined within the two-state manifolds of each well  $\{|e_i, n_i\rangle, |g_i, n_i + 1\rangle\}$  by a simple extension of the familiar solution to the Jaynes-Cummings model. Within each manifold the system undergoes Rabi oscillations.

Since tunneling is neglected during the photo-association steps, the two wells are independent of each other and identical to each other. The resultant molecular gain is then modeled by independent coarse-grained equations of motion for the reduced density matrices of each molecular mode.

(iv) The unitary time evolution of the molecular field under the influence of two-body collisions and quantum tunneling, a process absent in conventional micromasers. During the intervals  $T$  it is governed by

$$\frac{\partial \hat{\rho}_b}{\partial t} = -\frac{i}{\hbar}[\hat{H}_b, \hat{\rho}_b], \quad (9)$$

where the Hamiltonian

$$\hat{H}_b = -\hbar J_b(\hat{b}_l^\dagger \hat{b}_r + \hat{b}_r^\dagger \hat{b}_l) + \hbar \frac{U_b}{4}(\hat{n}_l - \hat{n}_r)^2 \quad (10)$$

contains tunneling and collisions. In Eq. (10), we have neglected terms that are functions only of  $\hat{N} = \hat{n}_l + \hat{n}_r$ , a step justified as long as the initial density matrix is diagonal in the total number of molecules in the two wells.

Combining the coherent and incoherent processes (i) to (iv), we obtain the full evolution of the molecular field

$$\frac{\partial \hat{\rho}_b}{\partial t} = \sum_{l,r} \mathcal{L}_i \hat{\rho}_b + \frac{1}{T} \sum_{l,r} [F_i(\tau) - I_i] \hat{\rho}_b - \frac{i}{\hbar} [H_b, \hat{\rho}_b], \quad (11)$$

where  $\hat{\rho}_b$  is the reduced density matrix of the molecules. The initial condition for the molecules is taken to be the vacuum state. Because the molecular pumping and decay is the same in both wells, the density matrix  $\rho$  remains diagonal in the total number of molecules in the two wells for all times. This is a generalization of the micromaser result that the photon density matrix will remain diagonal if it is initially diagonal in a number state basis (Filipowicz et al., 1986).

## B. Results

The master equation describing the molecular micromaser dynamics contains six independent parameters: the number of photo-association cycles per lifetime of the molecule,  $N_{ex} = 1/\gamma T$ ; the ‘‘pump parameter’’  $\Theta = \sqrt{N_{ex}}|\chi|\tau$ ; the two-body collision strength and tunneling coupling strength per decay rate,  $u_b = U_b/\gamma$  and  $t_J = J_b/\gamma$ ; and finally, the detuning parameter  $\eta = (2\omega_f - \omega_b)/2|\chi|$  and the nonlinear detuning parameter  $\beta \equiv (2U_x - U_b)/2|\chi|$ .

In our model, the atomic and molecular level separations in the wells are required to be much larger than the relevant interaction energies,

$$\hbar\omega_b \gg U_b \langle \hat{n}_i \rangle (\langle \hat{n}_i \rangle - 1), \quad |\chi| \sqrt{\langle \hat{n}_i \rangle}, \quad (12)$$

$\langle \hat{n}_i \rangle$  being the average number of molecules in well  $i$ . A comparison with actual experimental parameters (Greiner et al., 2002a; Jaksch et al., 1998; Miyakawa et al., 2004) shows that these conditions are satisfied as long as the number of molecules doesn’t exceed 10. In addition, the neglect of inter-well tunneling and damping effects during the photo-association pulses requires that

$$\tau \ll J_b^{-1}, \gamma^{-1}. \quad (13)$$

This condition is satisfied in typical experiments.

In the remainder of this section, we discuss the dynamics of the molecular field obtained by direct numerical integration of the master equation with a Runge-Kutta algorithm until a dissipative steady state is reached. For simplicity, we confine our discussion to exact resonance only,  $\eta = \beta = 0$ , and a fixed value of  $N_{ex} = 10$ .

### 1. single-well molecular statistics

We first discuss the statistics of a single-well molecular mode, which is given by tracing over the full density matrix with respect to degrees of freedom of the other localized mode as

$$P(n_{l\{r\}}) = Tr_{r\{l\}}[\rho(n_l, n_r; m_l, m_r)] = \sum_{n_r\{l\}} \rho(n_l, n_r; n_l, n_r). \quad (14)$$

We note that off-diagonal elements of the density matrix for a single well are zero. Since the initial state of the molecules in each well is the same, i.e. the vacuum state, and  $\hat{H}_b$  is invariant with respect to the interchange  $l \leftrightarrow r$ , the molecule statistics for left and right wells are identical,  $P(n_l) = P(n_r) \equiv P(n)$ .

Figure 1 shows the steady-state average number  $\langle \hat{n}_i \rangle$  is plotted as a function of the pump parameter  $\Theta$  for  $u_b = 0$ ,  $N_{ex} = 10$ . In the absence of inter-well tunneling, corresponding to Fig. 1(a), the result reproduces that of conventional micromasers, with a “lasing” threshold behavior at around  $\Theta \approx 1$  and an abrupt jump to a higher mean occupation at about the first transition point,  $\Theta \simeq 2\pi$ . The former effect is not affected by the tunneling coupling as shown in Fig. 1(b). However, the latter abrupt jump disappears in the presence of interwell tunneling. This is because the coupling to the other well leads to fluctuations in the number of molecules in each well and has an effect similar to thermal fluctuations in the traditional micromaser theory. The enhancement of fluctuations can also be seen in Fig. 2 where the Mandel  $Q$ -parameter

$$Q = \frac{\langle \hat{n}_i^2 \rangle - \langle \hat{n}_i \rangle^2}{\langle \hat{n}_i \rangle} - 1$$

is plotted as a function of  $\Theta$ .

It is known that in the usual micromaser the sharp resonance-like dips in  $\langle \hat{n}_i \rangle$  and  $Q$  are attributable to trapping states, which are characterized by a sharp photon number. For the specific value of  $\Theta = \sqrt{5}\pi$ , as shown in Fig. 3(a), the number probability does not reach beyond number state  $|n_i = 1\rangle$  in the case of  $t_J = 0$ . As shown in Fig. 3(b), the tunneling coupling makes possible transitions into higher number states and eliminates the trapping state in a manner similar to thermal fluctuations in the conventional micro maser.

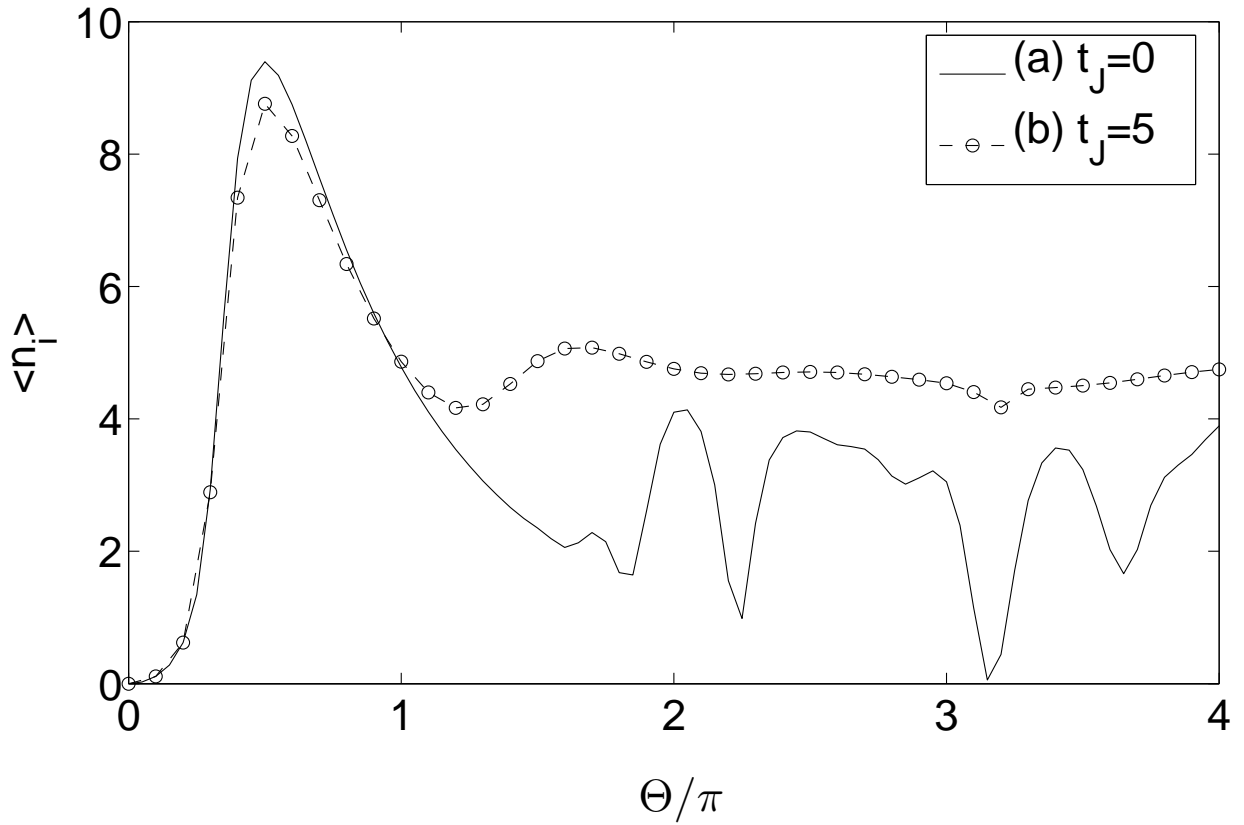


FIG. 1  $\langle \hat{n}_i \rangle$  versus  $\Theta/\pi$  for  $u_b = 0$  and  $N_{ex} = 10$ , and for (a)  $t_J = 0$  and (b)  $t_J = 5$ .

## 2. phase coherence between two micromasers with tunneling coupling

So far we have discussed the single-well molecule statistics and how it is affected by inter-well tunneling. Now we turn to a more detailed discussion of the phase coherence between the two localized modes. It is very useful to divide the parameter space of the ratio of the two-body collision strength to the inter-well tunneling coupling into three regimes (Leggett, 2001): “Rabi-regime” ( $u_b/t_J \ll \langle \hat{N} \rangle^{-1}$ ); “Josephson-regime” ( $\langle \hat{N} \rangle^{-1} \ll u_b/t_J \ll \langle \hat{N} \rangle$ ); and “Fock-regime” ( $\langle \hat{N} \rangle \ll u_b/t_J$ ); where  $\langle \hat{N} \rangle$  denotes the average total molecule number.

The analysis of the relative coherence of the molecular fields in the two wells is most conveniently discussed in terms of the angular momentum representation

$$\begin{aligned}
 \hat{J}_+ &= \hat{J}_x + i\hat{J}_y = \hat{b}_l^\dagger \hat{b}_r, \\
 \hat{J}_- &= \hat{J}_x - i\hat{J}_y = \hat{b}_r^\dagger \hat{b}_l, \\
 \hat{J}_z &= \frac{1}{2}(\hat{b}_l^\dagger \hat{b}_l - \hat{b}_r^\dagger \hat{b}_r), \\
 \hat{J}^2 &= \frac{\hat{N}}{2} \left( \frac{\hat{N}}{2} + 1 \right).
 \end{aligned} \tag{15}$$

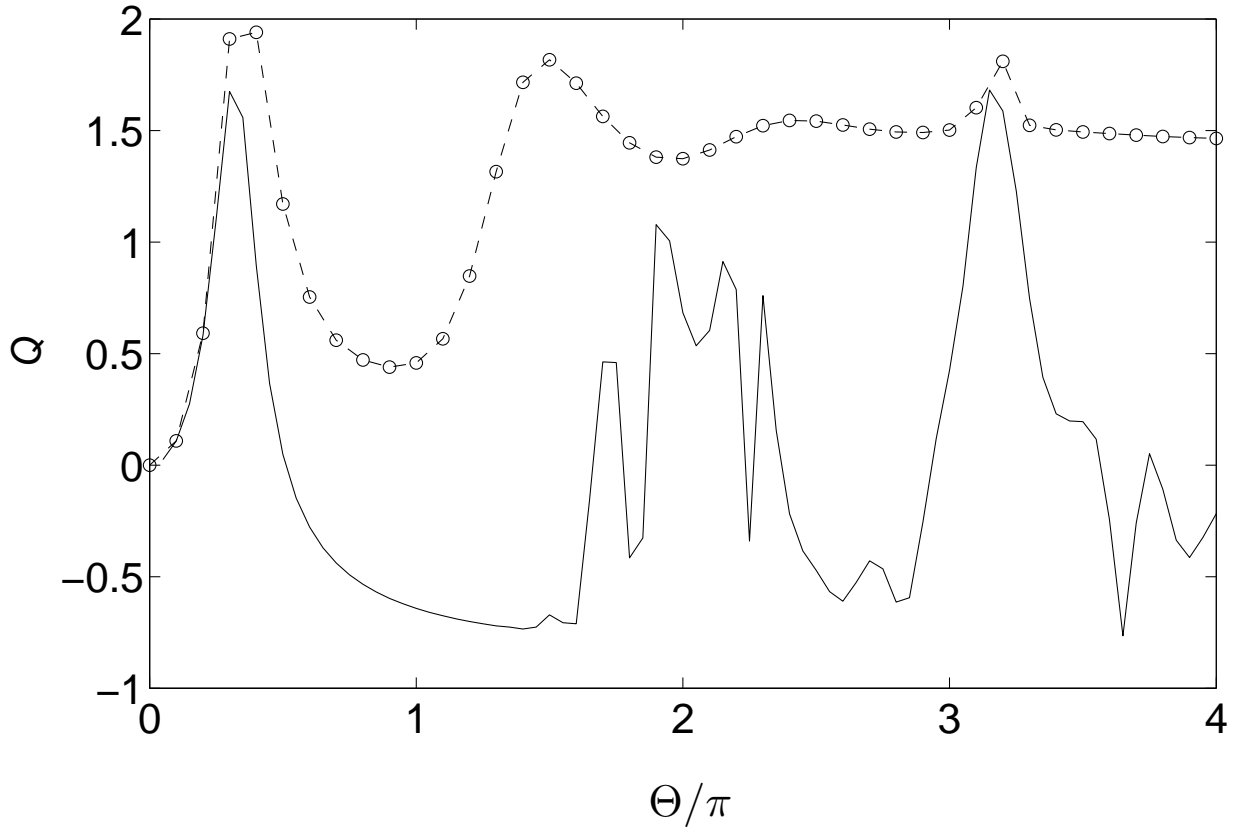


FIG. 2  $Q$  parameter versus  $\Theta/\pi$  for  $u_b = 0$  and  $N_{ex} = 10$ , and for (a)  $t_J = 0$  and (b)  $t_J = 5$ .

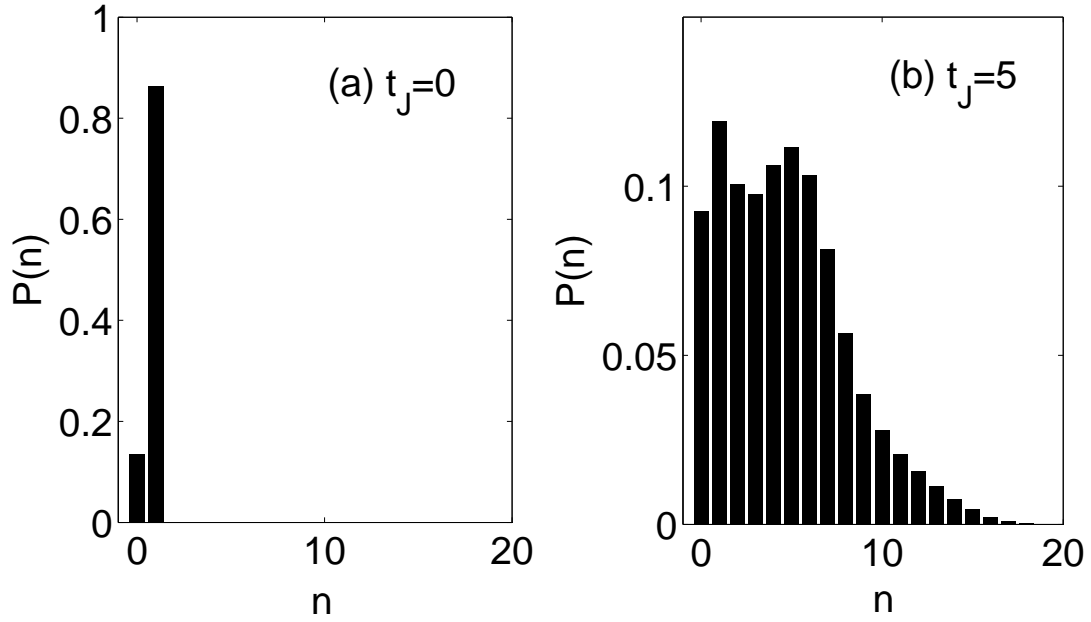


FIG. 3 Molecular number statistics  $P(n_i)$  for  $\Theta = \sqrt{5}\pi$ ,  $u_b = 0$  and  $N_{ex}$ , and for (a)  $t_J = 0$  and (b)  $t_J = 5$ .

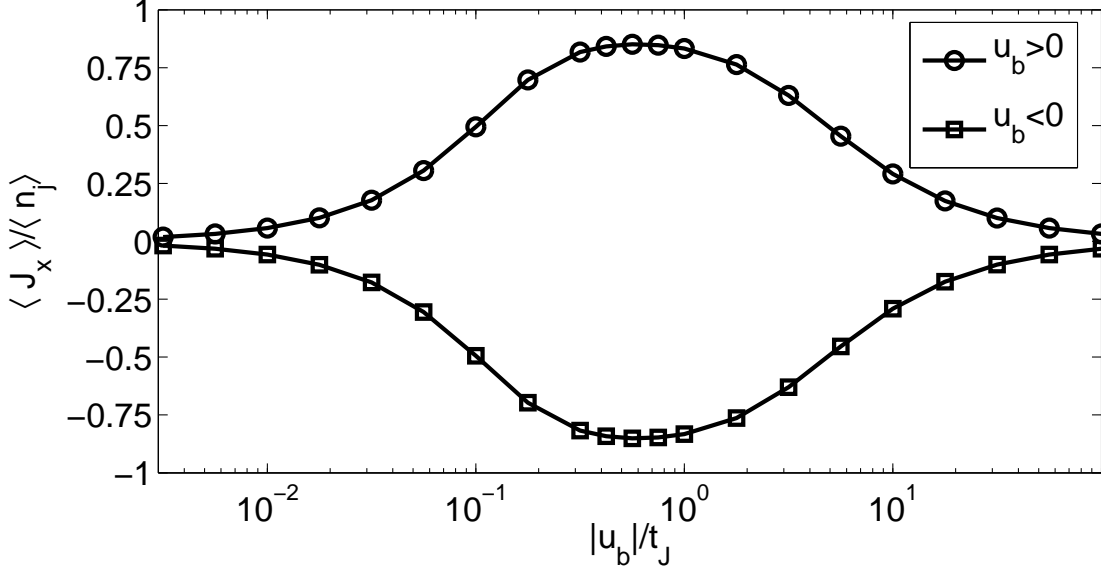


FIG. 4  $\langle \hat{J}_x \rangle / \langle \hat{n}_j \rangle$  versus  $u_b/t_J$  for  $\Theta = \pi$  and  $t_J = 2.5$ .

The symmetry of the density matrix with respect to the two wells furthermore implies that  $\langle \hat{J}_z \rangle = \langle \hat{J}_y \rangle = 0$ . The first-order coherence between the molecular fields in the left and right potential wells is then given by  $\langle \hat{J}_x \rangle$ . Figure 4 shows the normalized steady-state first-order coherence  $\langle \hat{J}_x \rangle / \langle \hat{n}_j \rangle$  as a function of  $u_b/t_J$  for  $\Theta = \pi$  and  $t_J = 2.5$ .  $\langle \hat{J}_x \rangle$  is suppressed in both the Rabi and Fock regimes and has an extremum at  $|u_b|/t_J \sim 0.6$ . In the Fock regime,  $|u_b|/t_J \gg \langle \hat{N} \rangle \sim 10$ , the nonlinearity in  $\hat{H}_b$  dominates and reduces the coherence between the localized states of each well. We note that the average occupation numbers for each well are relatively unaffected by  $u_b/t_J$ , with  $\langle \hat{n}_j \rangle = \langle \hat{N} \rangle / 2 = 4.78 - 4.87$  for  $|u_b|/t_J = 10^2 - 10^{-2.5}$ .

The reason why the first-order coherence is suppressed in the weak coupling limit,  $u_b = 0$ , can be understood as follows. The expectation value  $\langle \hat{J}_x \rangle$  corresponds to the difference in occupation numbers between the in-phase,  $\hat{b}_s = (\hat{b}_l + \hat{b}_r)/\sqrt{2}$ , and out-of-phase,  $\hat{b}_a = (\hat{b}_l - \hat{b}_r)/\sqrt{2}$ , states of the localized states of each well,  $\hat{J}_x = \hat{b}_s^\dagger \hat{b}_s - \hat{b}_a^\dagger \hat{b}_a$ . Since the bandwidth of the photo-association pulse is larger than their energy splitting,  $1/\tau \gg J_b$ , those states are equally populated, resulting in  $\langle \hat{J}_x \rangle = 0$  for  $u_b = 0$ . Thus, the origin of the mutual coherence between two molecular modes is due solely to two-body collisions. Furthermore, we remark that a semiclassical treatment results in  $\langle \hat{J}_x \rangle = 0$  for all times and all values of  $u_b/t_J$  (Miyakawa et al., 2004). Hence, we conclude that the build-up of  $\langle \hat{J}_x \rangle$  is a purely quantum-mechanical effect due to quantum fluctuations.

The phase distribution of the two wells can be studied using the Pegg-Barnett phase states (Barnett and Pegg,

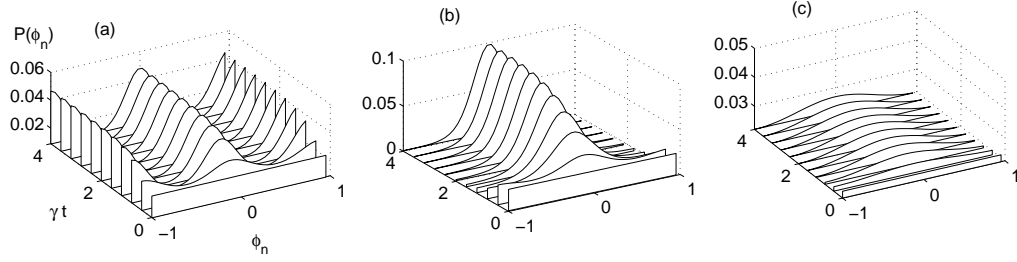


FIG. 5 Time evolution of  $P(\phi_n)$  for  $\Theta = \pi$ ,  $t_J = 2.5$  and for (a)  $u_b/t_J = 0.0032$ , (b)  $u_b/t_J = 0.5623$ , (c)  $u_b/t_J = 56.23$ .

1990; Javanainen and Ivanov, 1999; Luis and Sanchez-Soto, 1993; Pegg and Barnett, 1988). Since the density matrix is diagonal in the total number of molecules it is sufficient to consider the relative phase. Figure 5 shows the time evolution of the relative phase distribution in three different regimes: (a) Rabi,  $u_b/t_J = 0.0032$ , (b) Josephson,  $u_b/t_J = 0.5623$ , and (c) Fock  $u_b/t_J = 56.23$ , for  $\Theta = \pi$ ,  $t_J = 2.5$ . Since the vacuum state is taken as the initial state, the relative phase at  $t = 0$  is randomly distributed,  $P(\phi_n) = 1/(s + 1)$ .

In the Rabi regime, corresponding to Fig.5(a), bimodal phase distribution with peaks around both 0 and  $\pm\pi$  builds up in the characteristic time  $\gamma^{-1}$  needed to reach a steady state (Filipowicz et al., 1986). In the Josephson regime, the relative phase locks around 0 ( $\pm\pi$ ), for repulsive (attractive) two-body interactions, see Fig. 5(b). In contrast to these two regimes, in the Fock regime the relative phase distribution becomes almost random for all times, and the localized modes in the two wells evolve independently of each other.

The three regimes of phase distributions correspond to different orders of magnitude of the ratio  $u_b/t_J$ . The crossover of the non-equilibrium steady state from a phase-coherent regime to the random-phase situation is reminiscent of the superfluid-Mott insulator phase transition for the ground state of an optical lattice (Fisher et al., 1989; Jaksch et al., 1998). Since we consider just two sites, however, there is no sharp transition between these regimes.

### III. PASSAGE TIME STATISTICS OF MOLECULE FORMATION

We now turn to a second-example that illustrates the understanding of the dynamics of quantum-degenerate atomic and molecular systems that can be gained from quantum optics analogies. Here, we consider the first stages of coherent

molecular formation via photo-association. Since in such experiments the molecular field is typically in a vacuum initially, it is to be intuitively expected that the initial stages of molecule formation will be strongly governed by quantum noise, hence subject to large fluctuations. One important way to characterize these fluctuations is in terms of the so-called passage time, which is the time it takes to produce, or dissociate, a predetermined number of molecules. Quantum noise results in fluctuations in that time, whose probability distribution can therefore be used to probe the fluctuations in the formation dynamics.

Because of the analogy between pairs of fermionic atoms and two-level systems that we already exploited in the discussion of the molecular micromaser, one can expect that the problem at hand is somewhat analogous to spontaneous radiation from a sample of two-level atoms, the well-know problem of superradiance. In this section we show that this is indeed the case, and use this analogy to study the passage time statistics of molecular formation from fermionic atoms.

### A. Model

We consider again a quantum-degenerate gas of fermionic atoms of mass  $m_f$  and spin  $\sigma = \uparrow, \downarrow$ , coupled coherently to bosonic molecules of mass  $m_b = 2m_f$  and zero momentum via photo-association. Neglecting collisions between fermions and assuming that for short enough times the molecules occupy a single-mode of the bosonic field, this system can be described by the boson-fermion model Hamiltonian

$$H = \sum_k \frac{1}{2} \hbar \omega_k \left( \hat{c}_{k\uparrow}^\dagger \hat{c}_{k\uparrow} + \hat{c}_{-k\downarrow}^\dagger \hat{c}_{-k\downarrow} \right) + \hbar \omega_b \hat{b}^\dagger \hat{b} + \hbar \chi \sum_k \left( \hat{b}^\dagger \hat{c}_{k\uparrow} \hat{c}_{-k\downarrow} + \hat{b} \hat{c}_{-k\uparrow}^\dagger \hat{c}_{k\downarrow}^\dagger \right), \quad (16)$$

where  $\hat{b}^\dagger, \hat{b}$  are molecular bosonic creation and annihilation operators and  $\hat{c}_{k\sigma}^\dagger, \hat{c}_{k\sigma}$  are fermionic creation and annihilation operators describing atoms of momentum  $\hbar k$  and spin  $\sigma$ . The first and second terms in Eq. (16) describe the kinetic energy  $\hbar \omega_k / 2 = \hbar^2 k^2 / (2m_f)$  of the atoms and the detuning energy of the molecules respectively, and the third term describes the photo-association of pairs of atoms of opposite momentum into molecules.

Introducing the pseudo-spin operators (Anderson, 1958) analogous to Eq. (7)

$$\begin{aligned} \hat{\sigma}_k^z &= \frac{1}{2} (\hat{c}_{k\uparrow}^\dagger \hat{c}_{k\uparrow} + \hat{c}_{-k\downarrow}^\dagger \hat{c}_{-k\downarrow} - 1), \\ \hat{\sigma}_k^+ &= (\hat{\sigma}_k^-)^\dagger = \hat{c}_{-k\downarrow}^\dagger \hat{c}_{k\uparrow}, \end{aligned} \quad (17)$$

the Hamiltonian (16) becomes, within an unimportant constant (Barankov and Levitov, 2004; Meiser and Meystre,

2005),

$$H = \sum_k \hbar\omega_k \hat{\sigma}_k^z + \hbar\omega_b \hat{b}^\dagger \hat{b} + \hbar\chi \sum_k \left( \hat{b}^\dagger \hat{\sigma}_k^- + \hat{b} \hat{\sigma}_k^+ \right). \quad (18)$$

This Hamiltonian is known in quantum optics as the inhomogeneously broadened (or non-degenerate) Tavis-Cummings model (Tavis and Cummings, 1968). It describes the coupling of an ensemble of two-level atoms to a single-mode electromagnetic field. Hence the mapping (17) establishes the formal analogy between the problem at hand and Dicke superradiance, with the caveat that we are dealing with a single bosonic mode (Andreev et al., 2004; Barankov and Levitov, 2004; Javanainen et al., 2004; Meiser and Meystre, 2005; Miyakawa and Meystre, 2005; Tikhonenkov and Vardi, 2004). Instead of real two-level atoms, pairs of fermionic atoms are now described as effective two-level systems whose ground state corresponds to the absence of a pair,  $|g_k\rangle = |0_{k\uparrow}, 0_{-k\downarrow}\rangle$  and the excited state to a pair of atoms of opposite momenta,  $|e_k\rangle = |1_{k\uparrow}, 1_{-k\downarrow}\rangle$ , in close analogy to the treatment of the atoms in the previous section.

The initial condition consists of the molecular field in the vacuum state and a filled Fermi sea of atoms

$$|F\rangle = \prod_{k \leq |k_F|} \hat{\sigma}_k^+ |0\rangle, \quad (19)$$

where  $k_F$  is the Fermi momentum. As such, the problem at hand is in direct analogy to the traditional superradiance problem where one starts from an ensemble of excited two-state atoms, as expected from our previous comments. Later on we will also consider an initial state containing only molecules and no atoms. This is an important extension of the traditional Dicke superradiance system, where the two-level atoms are coupled to all modes of the photon vacuum a situation, thereby precluding the possibility of an initial state containing a single, macroscopically occupied photon mode unless the system is prepared in a high- $Q$  cavity.

We assume from now on that the inhomogeneous broadening due to the spread in atomic kinetic energies can be ignored. This so-called degenerate approximation is justified provided that the kinetic energies are small compared to the atom-molecule coupling energy,  $\beta = \epsilon_F/(\hbar\chi) \ll 1$ , where  $\epsilon_F$  is the Fermi energy. It is the analog of the homogeneous broadening limit of quantum optics, and of the Raman-Nath approximation in atomic diffraction. A comparison with typical experimental parameters (Heinzen et al., 2000) shows that the degenerate approximation is justified if the number of atoms does not exceed  $\sim 10^2 - 10^3$  (Uys et al., 2005).

Limiting thus our considerations to small atomic samples, we approximate all  $\omega_k$ 's by  $\omega_F$  and introduce the collective

pseudo-spin operators

$$\begin{aligned}\hat{S}_z &= \sum_k \hat{\sigma}_k^z, \\ \hat{S}^\pm &= \sum_k \hat{\sigma}_k^\pm,\end{aligned}\tag{20}$$

obtaining the standard Tavis-Cummings Hamiltonian (Miyakawa and Meystre, 2005; Tavis and Cummings, 1968)

$$H = \hbar\omega_F \hat{S}_z + \hbar\omega_b \hat{b}^\dagger \hat{b} + \hbar\chi(\hat{b} \hat{S}^+ + \hat{b}^\dagger \hat{S}^-).\tag{21}$$

This Hamiltonian conserves the total spin operator  $\hat{S}^2$ . The total number of atoms is twice the total spin and hence is also a conserved quantity.  $\hat{S}_z$  measures the difference in the numbers of atom pairs and molecules.

Eq. (21) can be diagonalized numerically with reasonable computation times even for relatively large numbers of atoms. One can, however, gain significant intuitive insight in the underlying dynamics by finding operator equations of motion and then treating the short-time molecular population semiclassically,  $\langle \hat{n}_b \rangle \rightarrow n_b$ . To this end we introduce the ‘‘joint coherence’’ operators

$$\begin{aligned}\hat{T}_x &= (\hat{b} \hat{S}^+ + \hat{b}^\dagger \hat{S}^-)/2, \\ \hat{T}_y &= (\hat{b} \hat{S}^+ - \hat{b}^\dagger \hat{S}^-)/2i,\end{aligned}\tag{22}$$

and find the Heisenberg equations of motion

$$\dot{\hat{n}}_b = -2\chi \hat{T}_y,\tag{23}$$

$$\dot{\hat{T}}_x = \delta \hat{T}_y\tag{24}$$

$$\dot{\hat{T}}_y = -\delta \hat{T}_x - \chi (2\hat{S}_z \hat{n}_b + \hat{S}^+ \hat{S}^-),\tag{25}$$

where  $\delta = \omega_b - \omega_F$ , so that  $2\chi \hat{T}_x + \delta \hat{n}_b$  is a constant of motion.

In the following, we confine our discussion to the case of  $\delta = 0$  for simplicity. We thus neglect the contribution of  $\hat{T}_x$  in Eq. (25). In order to better understand the short time dynamics we reexpress  $\hat{S}^+ \hat{S}^-$  as

$$\hat{S}^+ \hat{S}^- = -\hat{n}_b^2 + (2S - 1)\hat{n}_b + N.\tag{26}$$

This shows that the operator  $\hat{S}^+ \hat{S}^-$  is non-vanishing when the molecular field is in a vacuum and hence can be interpreted as a noise operator. Indeed Eqs. (23)-(25) show that the buildup of the molecular field is triggered only by noise if  $\hat{n}_b = 0$  initially. By keeping only the lowest-order terms in  $\hat{n}_b$  we can eliminate  $\hat{T}_y$  to obtain the differential equation

$$\ddot{\hat{n}}_b \approx 2N\chi^2 (2\hat{n}_b + 1)\tag{27}$$

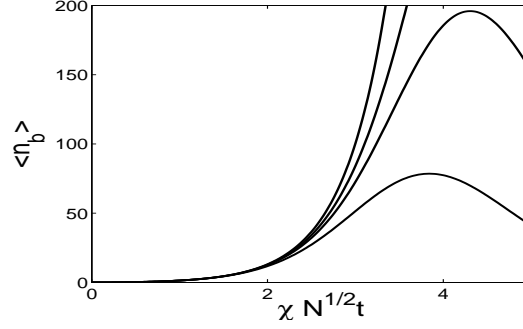


FIG. 6 Short-time dynamics of  $\langle \hat{n}_b \rangle$ . From left to right, the curves give the linearized solution (28) and the full quantum results for  $N = 500$ ,  $N = 250$ , and  $N = 100$ , respectively. Figure taken from Ref. (Uys et al., 2005)

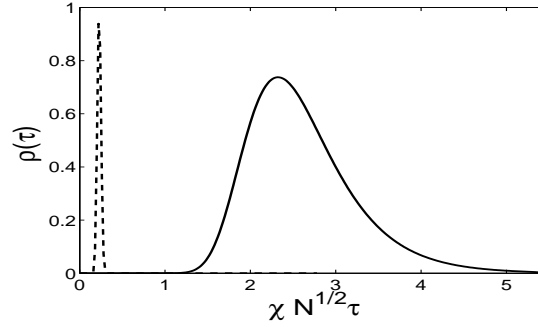


FIG. 7 Passage time distribution for converting 5% of the initial population consisting of only atoms (molecules) into molecules (atoms) for  $N = 500$ . For initially all atoms: solid line, for initially all molecules: dashed line.

which, for our initial state, may be solved to yield

$$\langle \hat{n}_b(t) \rangle \approx \sinh^2(\chi\sqrt{N}t). \quad (28)$$

Fig. 6 compares the average molecule number  $\langle \hat{n}_b \rangle$  obtained this way, with the full quantum solution obtained by direct diagonalization of the Hamiltonian (21) for various values of  $N$ . The semiclassical approach agrees within 5% of the full quantum solution until about 20% of the population of atom pairs has been converted into molecules in all cases.

Next we turn to the passage time statistics. In Fig 7 we show (solid line) the distribution of times required to produce a normalized molecule number  $n_b^{\text{ref}}/N = 0.05$  from a sample initially containing  $N = 500$  pairs of atomic fermions, as found by direct diagonalization of the Hamiltonian (21). This distribution differs sharply from its counterpart for the reverse process of photodissociation from a molecular condensate into fermionic atom pairs, which is plotted as the dashed line in Fig. 7. In contrast to photo-association, this latter process suffers significantly reduced fluctuations.

To understand the physical mechanism leading to this reduction in fluctuations we again turn to our short time

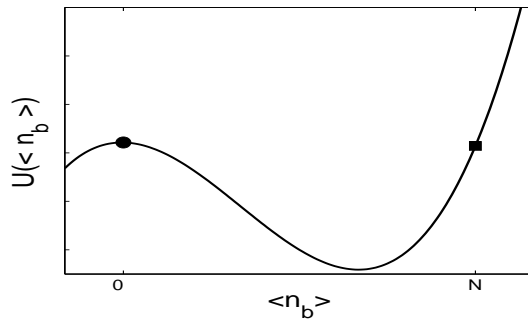


FIG. 8 Effective potential for a system with  $N \gg 1$ . The circle (square) corresponds to an initial state with all fermionic atoms (molecules). The part of the potential for  $n_b < 0$  is unphysical. Figure taken from Ref. (Uys et al., 2005)

semi-classical model. Within this approximation, the Heisenberg equations of motion (23)-(24) can be recast in the form of a Newtonian equation (Miyakawa and Meystre, 2005)

$$\frac{d^2 n_b}{dt^2} = -\frac{dU(n_b)}{dn_b}, \quad (29)$$

where the cubic effective potential  $U(n_b)$  is plotted in Fig. 8. (Note we have now kept all orders in  $n_b$ .) In case the system is initially composed solely of fermionic atoms,  $n_b(0) = 0$ , the initial state is dynamically unstable, with fluctuations having a large impact on the build-up of  $n_b$ . In contrast, when it consists initially solely of molecules,  $n_b = N$ , the initial state is far from the point of unstable equilibrium, and  $n_b$  simply “rolls down” the potential in a manner largely insensitive to quantum fluctuations. This is a consequence of the fact that the bosonic initial state provides a mean field that is more amenable to a classical description. Hence, while the early stages of molecular dimer formation from fermionic atoms are characterized by large fluctuations in formation times that reflect the quantum fluctuations in the initial atomic state, the reverse process of dissociation of a condensate of molecular dimers is largely deterministic. The diminished fluctuations in this reversed process is peculiar to the atom-molecule system and not normally considered in the quantum optics analog of Dicke superradiance.

#### IV. COUNTING STATISTICS OF MOLECULAR FIELDS

An important quantum mechanical characteristic of a quantum field is its counting (or number) statistics. In this section we show how the similarity of the coherent molecule formation with quantum optical sum-frequency generation can be used to determine the counting statistics of the molecular field. In particular we show how the counting statistics depends on the statistics of the atoms from which the molecules are formed. Besides being interesting in its own right, such an analysis is crucial for an understanding of several recent experiments that used a “projection” onto molecules

to detect BCS superfluidity in fermionic systems (Regal et al., 2004a; Zwierlein et al., 2004). Our work shows that the statistical properties of the resulting molecular field indeed reflect properties of the initial atomic state and are a sensitive probe for superfluidity.

As before, we restrict our discussion to a simple model in which all the molecules are generated in a single mode. We use time dependent perturbation theory to calculate the number of molecules formed after some time  $t$ ,  $n(t)$ , as well as the equal-time second-order correlation function  $g^{(2)}(t, t)$ . We also integrate the Schrödinger equation numerically for small numbers of atoms, which allows us to calculate the complete counting statistics  $P_n$ .

### A. BEC

Consider first a cloud of weakly interacting bosons well below the condensation temperature  $T_c$ . It is a good approximation to assume that all atoms are in the condensate, described by the condensate wave function  $\psi_0(x)$ . The coupled system of atoms and molecules is described by the effective two-mode Hamiltonian (Anglin and Vardi, 2001; Javanainen and Mackie, 1999)

$$\hat{H}_{\text{BEC}} = \hbar\delta\hat{b}^\dagger\hat{b} + \hbar\chi\left(\hat{b}^\dagger\hat{c}^2 + \hat{b}\hat{c}^{\dagger 2}\right). \quad (30)$$

where  $\hat{b}$ ,  $\hat{b}^\dagger$  and  $\hat{c}$ ,  $\hat{c}^\dagger$  are the bosonic annihilation and creation operators for the molecules and for the atoms in the condensate, respectively,  $\delta$  is the detuning between the molecular and atomic level, and  $\hbar\chi$  is the effective coupling constant.

Typical experiments start out with all atoms in the condensate and no molecules, corresponding to the initial state,

$$|\psi(t=0)\rangle = \frac{\hat{c}^{\dagger N_a}}{\sqrt{N_a!}}|0\rangle. \quad (31)$$

where  $N_a = 2N_{\text{max}}$  is the number of atoms,  $N_{\text{max}}$  is the maximum possible number of molecules and  $|0\rangle$  is the vacuum of both molecules and atoms. We can numerically solve the Schrödinger equation for this problem in a number basis and from that solution we can determine the molecule statistics  $P_n(t)$ . The results of such a simulation are illustrated in Fig. 9, which shows  $P_n(t)$  for 30 initial atom pairs and  $\delta = 0$ . Starting in the state with zero molecules, a wave-packet-like structure forms and propagates in the direction of increasing  $n$ . Near  $N_{\text{max}}$  the molecules begin to dissociate back into atom pairs.

We can gain some analytical insight into the short-time dynamics of molecule formation by using first-order per-

turbation theory (Kozierowski and R. Tanaś, 1977; Mandel, 1982). We find for the mean molecule number

$$n(t) = (\chi t)^2 2N_{\max}(2N_{\max} - 1) + \mathcal{O}((\chi t)^2) \quad (32)$$

and for the second factorial moment

$$g^{(2)}(t_1, t_2) = 1 - \frac{2}{N_{\max}} + \mathcal{O}(N_{\max}^{-2}). \quad (33)$$

For  $N_{\max}$  large enough we have  $g^{(2)}(t_1, t_2) \rightarrow 1$ , the value characteristic of a Glauber coherent field. From  $g^{(2)}$  and  $n(t)$  we also find the relative width of the molecule number distribution as

$$\frac{\sqrt{\langle(\hat{n} - n)^2\rangle}}{n} = \sqrt{g^{(2)} + n^{-1} - 1}. \quad (34)$$

It approaches  $n^{-1/2}$  in the limit of large  $N_{\max}$ , typical of a Poisson distribution. This confirms that for short enough times, the molecular field is coherent in the sense of quantum optics.

## B. Normal Fermi gas

We now turn to the case of photo-association from two different species of non-interacting ultra-cold fermions. The two species are again denoted by spin up and down. At  $T = 0$ , the atoms fill a Fermi sea up to an energy  $\mu$ . Weak repulsive interactions give rise only to minor quantitative modifications that we ignore. We refer to this system of non-interacting Fermions as a normal Fermi gas (NFG) (Landau et al., 1980).

As before we assume that atom pairs are coupled only to a single mode of the molecular field, which we assume to have zero momentum for simplicity. Then, using the mapping to pseudo spins Eq. (17) we find that the system is again described by the inhomogeneously broadened Tavis-Cummings Hamiltonian Eq. (18). However, in contrast to the previous case, we do not assume that the fermionic energies are approximately degenerate, in order to be able compare the results to the BCS case, where the kinetic energies are essential.

Figure 10 shows the molecule statistics obtained this way. The result is clearly both qualitatively and quantitatively very different from the case of molecule formation from an atomic BEC. From the Tavis-Cummings model analogy we expect that for short times the statistics of the molecular field should be chaotic, or “thermal”, much like those of a single-mode chaotic light field. This is because each individual atom pair ”emits” a molecule independently and without any phase relation with other pairs. That this is the case is illustrated in the inset of Fig. 10, which fits the molecule statistics at selected short times with chaotic distributions of the form

$$P_{n,\text{thermal}} = \frac{e^{-n/\langle n \rangle}}{\sum_n e^{-n/\langle n \rangle}}. \quad (35)$$

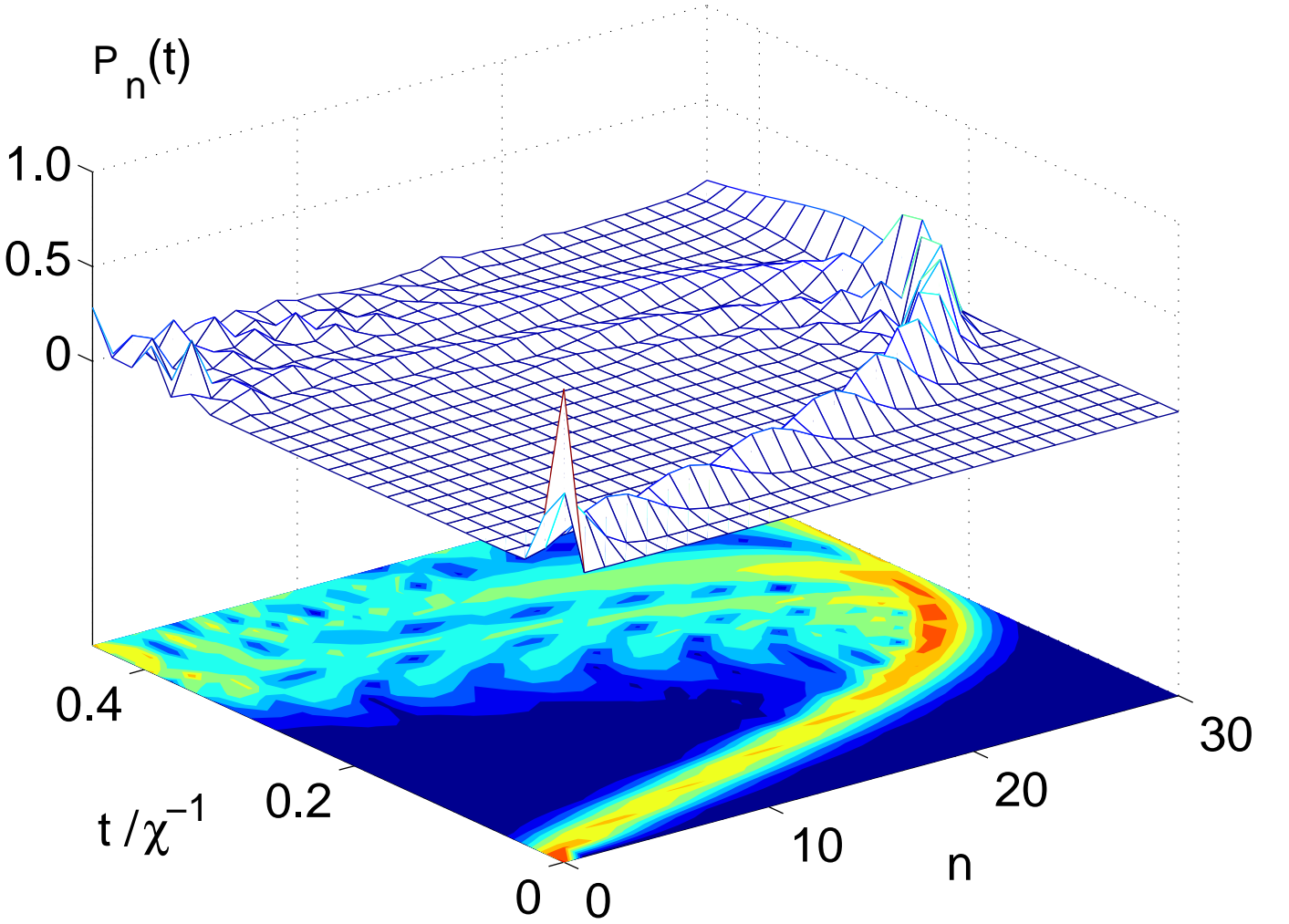


FIG. 9 Number statistics of molecules formed from a BEC with  $N_{\max} = 30$  and  $\delta = 0$ .

The increasing ‘pseudo-temperature’  $\langle n \rangle$  corresponds to the growing average number of molecules as a function of time.

As before we determine the short-time properties of the molecular field in first-order perturbation theory. We find for the mean number of molecules

$$n(t) = (\chi t)^2 2N_a. \quad (36)$$

It is proportional to  $N_a$ , in contrast to the BEC result, where  $n$  was proportional to  $N_a^2$ , see Eq. (32). This is another manifestation of the independence of all the atom pairs from each other: While in the BEC case the molecule production is a collective effect with contributions from all possible atom pairs adding constructively, there is no such collective enhancement in the case of Fermions. Each atom can pair up with only one other atom to form a molecule.

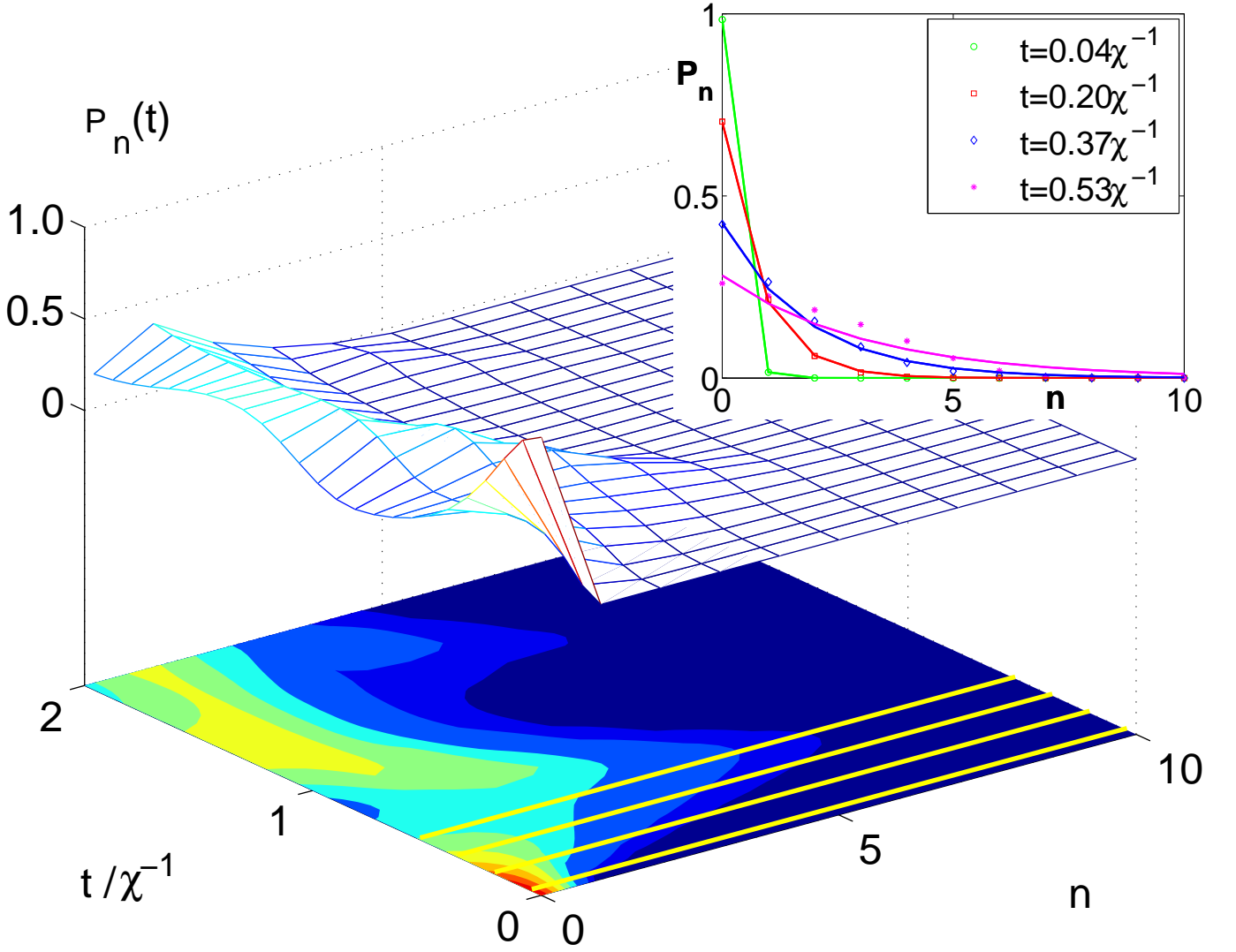


FIG. 10 Number statistics of molecules formed from a normal Fermi gas. This simulation is for  $N_a = 20$  atoms, the detuning is  $\delta = 0$ , the Fermi energy is  $\mu = 0.1\hbar\chi$  and the momentum of the  $i$ -th pair is  $|k_i| = (i - 1)2k_F/(N_a/2 - 1)$ . The inset shows fits of the number statistics to thermal distributions for various times as marked by the thick lines in the main figure.

For the second factorial moment we find

$$g^{(2)}(t_1, t_2) = 2 \left( 1 - \frac{1}{2N_a} \right) \quad (37)$$

which is close to two, typical of a chaotic or thermal field.

### C. Fermi gas with superfluid component

Unlike repulsive interactions, attractive interactions between fermions have a profound impact on molecule formation. It is known that such interactions give rise to a Cooper instability that leads to pairing and drastically changes

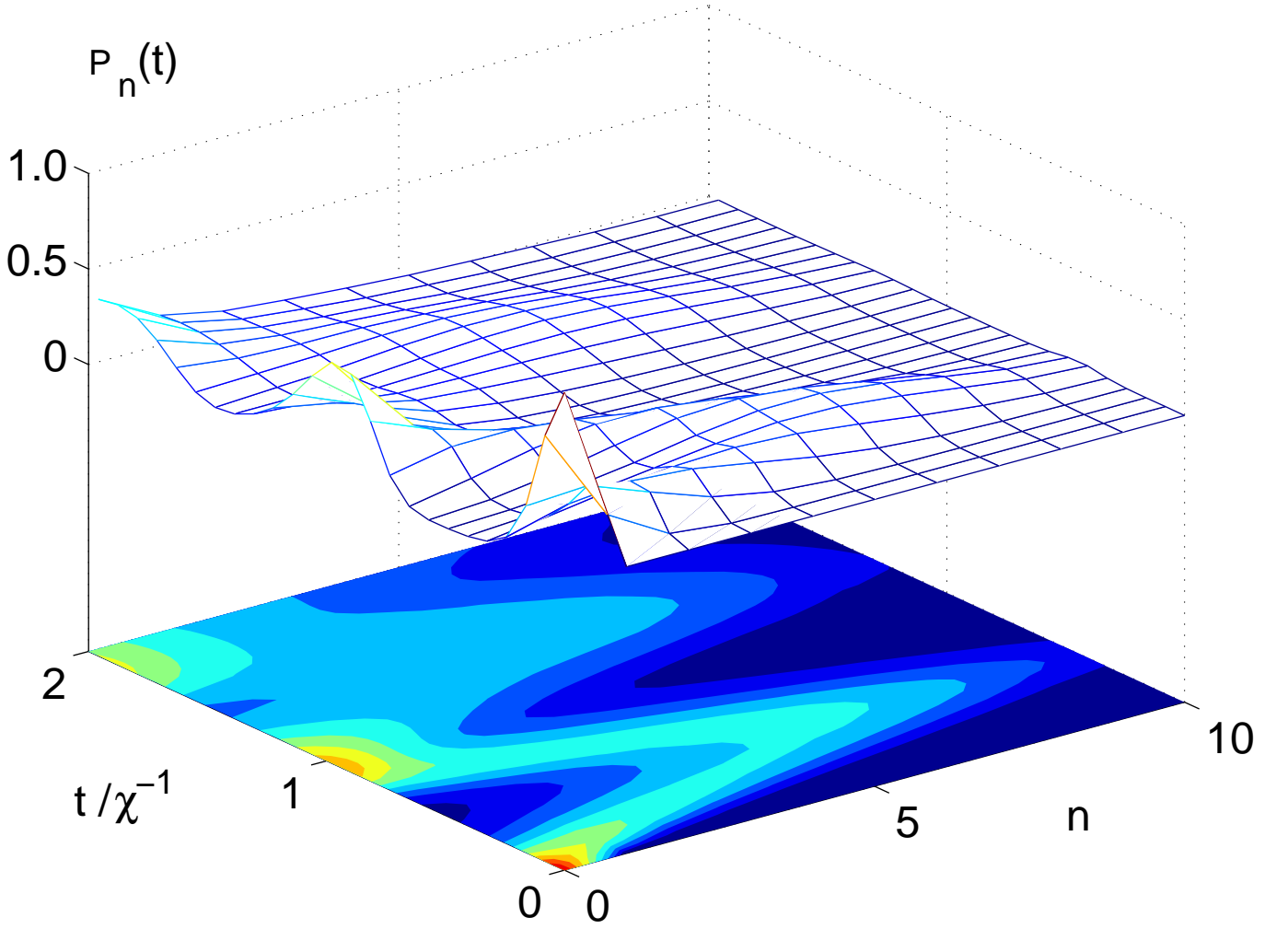


FIG. 11 Number statistics of molecules formed from a Fermi gas with pairing correlations. For this simulation the detuning is  $\delta = 0$ , the Fermi energy is  $\mu = 0.1g$  and the background scattering strength is  $V = 0.03\chi$  resulting in  $N_a \approx 9.4$  atoms and a gap of  $\Delta \approx 0.15\chi$ . The momenta of the atom pairs are distributed as before in the normal Fermi gas case.

the qualitative properties of the atomic system. The BCS reduced Hamiltonian is essentially the inhomogeneously broadened Tavis-Cummings Hamiltonian (18) with an additional term accounting for the attractive interactions between atoms (Kittel, 1987),

$$H = \sum_k \hbar\omega_k \hat{\sigma}_k^z + \hbar\omega_b \hat{b}^\dagger \hat{b} + \hbar\chi \sum_k \left( \hat{b}^\dagger \hat{\sigma}_k^- + \hat{b} \hat{\sigma}_k^+ \right) - V \sum_{k,k'} \hat{\sigma}_k^+ \hat{\sigma}_{k'}^- . \quad (38)$$

The approximate mean-field ground state  $|BCS\rangle$  is found by minimizing  $\langle \hat{H}_{BCS} - \mu \hat{N} \rangle$  in the standard way. The dynamics is then obtained by numerically integrating the Schrödinger equation with  $|BCS\rangle$  as the initial atomic state and the molecular field in the vacuum state.

Figure 11 shows the resulting molecule statistics for  $V = 0.03\hbar\chi$ , which corresponds to a gap of  $\Delta = 0.15\hbar\chi$  for the system at hand. Clearly, the molecule production is much more efficient than it was in the case of a normal Fermi

gas. The molecules are produced at a higher rate and the maximum number of molecules is larger. The evolution of the number statistics is reminiscent of the BEC case. This also shows that the qualitative differences seen between the normal Fermi gas and a BEC in the previous section cannot be attributed to inhomogeneous broadening and the resulting dephasing alone but are instead a result of the different coherence properties of the atoms.

The short-time dynamics is again obtained in first-order perturbation theory, which gives now

$$n(t) \approx (\chi t)^2 \left[ \left( \frac{\Delta}{V} \right)^2 + N_a \right]. \quad (39)$$

In addition to the term proportional to  $N_a$  representing the incoherent contribution from the individual atom pairs that was already present in the normal Fermi gas, there is now an additional contribution proportional to  $(\Delta/V)^2$ . Since  $(\Delta/V)$  can be interpreted as the number of Cooper pairs in the quantum-degenerate Fermi gas, this term can be understood as resulting from the *coherent* conversion of Cooper pairs into molecules in a collective fashion similar to the BEC case. The coherent contribution results naturally from the nonlinear coupling of the atomic field to the molecular field. This nonlinear coupling links higher-order correlations of the molecular field to lower-order correlations of the atomic field. For the parameters of Fig. 11  $\Delta/V \approx 6.5$  so that the coherent contribution from the Cooper pairs clearly dominates over the incoherent contribution from the unpaired fermions. Note that no signature of that term can be found in the momentum distribution of the atoms themselves. Their momentum distribution is very similar to that of a normal Fermi gas. The short-time value of  $g^{(2)}(t_1, t_2)$ , shown in Fig. 12, decreases from the value of Eq. (37) for a normal Fermi gas at  $\Delta = 0$  down to one as  $\Delta$  increases, underlining the transition from incoherent to coherent molecule production.

## V. MOLECULES AS PROBES OF SPATIAL CORRELATIONS

The single-mode description of the molecular field of the previous section results in the loss of all information about the spatial structure of the atomic state. In this final section we adopt a complementary view and study the coupled atom-molecule system including all modes of the molecular and atomic field so as to resolve their spatial structure. This problem is too complex to admit an exact solution, hence we rely entirely on perturbation theory.

One of the motivations for such studies is the on-going experimental efforts to study the so-called BEC-BCS crossover. A difficulty of these studies has been that they necessitate the measurement of higher-order correlations of the atomic system. While the momentum distribution of a gas of bosons provides a clear signature of the presence of a Bose-Einstein condensate, the Cooper pairing between fermionic atoms in a BCS state hardly changes the momentum

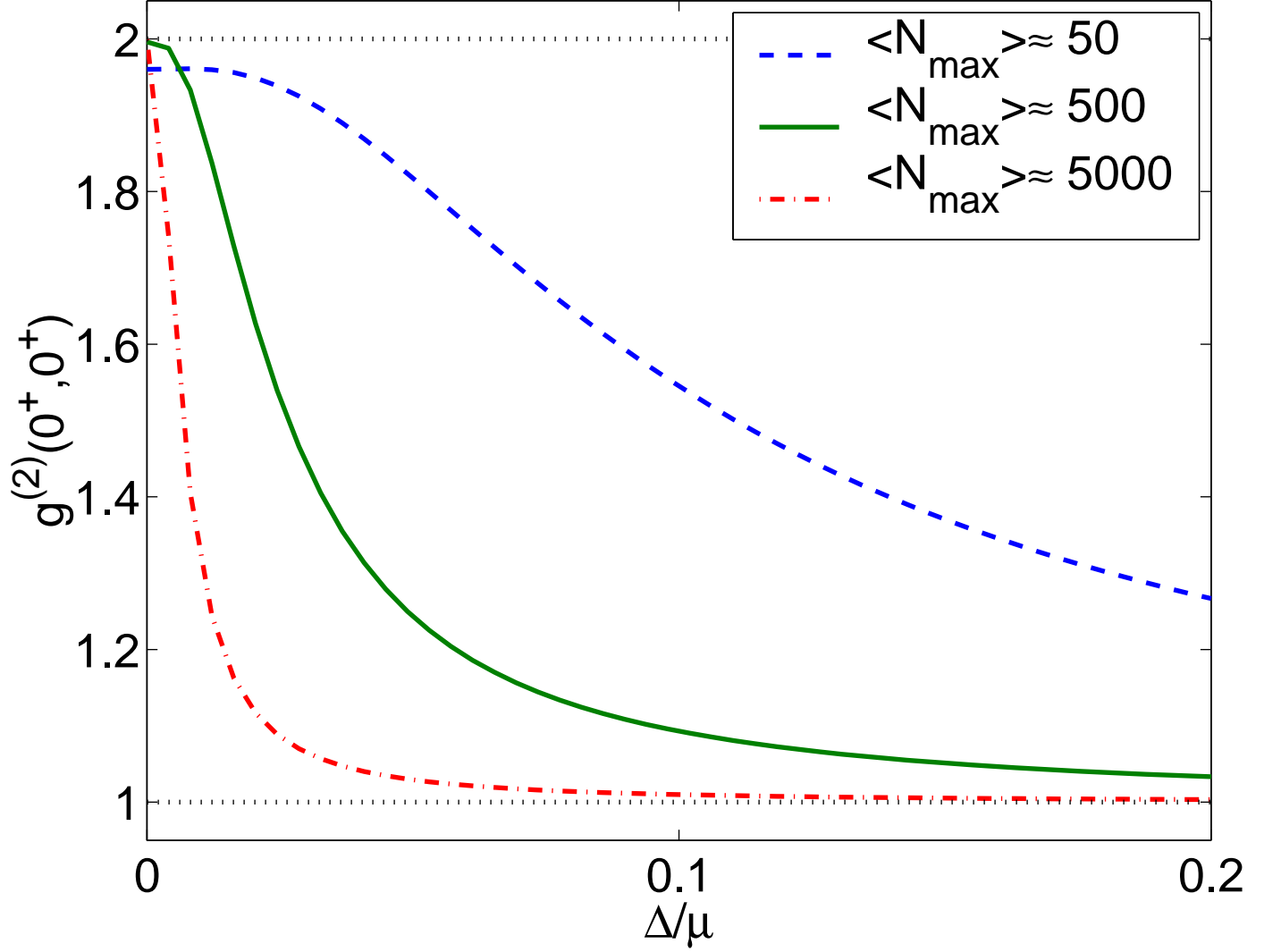


FIG. 12  $g^{(2)}(0^+, 0^+)$  as a function of the gap parameter  $\Delta$ . (Figure taken from Ref. (Meiser and Meystre, 2005))

distribution or spatial profile as compared to a normal Fermi gas. This poses a significant experimental challenge, since the primary techniques for probing the state of an ultra-cold gas are either optical absorption or phase contrast imaging, which directly measure the spatial density or momentum distribution following ballistic expansion of the gas. In the strongly interacting regime very close to the Feshbach resonance, evidence for fermionic superfluidity was obtained by projecting the atom pairs onto a molecular state by a rapid sweep through the resonance (Regal et al., 2004b; Zwierlein et al., 2004). More direct evidence of the gap in the excitation spectra due to pairing was obtained by rf spectroscopy (Chin et al., 2004) and by measurements of the collective excitation frequencies (Bartenstein et al., 2004; Kinast et al., 2004). Finally, the superfluidity of ultra-cold fermions in the strongly interacting regime has recently been impressively demonstrated via the generation of atomic vortices (Zwierlein et al., 2005).

Still, the detection of fermionic superfluidity in the weakly interacting BCS regime remains a challenge. The direct detection of Cooper pairing requires the measurement of second-order or higher atomic correlation functions. Several researchers have proposed and implemented schemes that allow one to measure higher order correlations (Altman et al., 2004; Bach and Rzażewski, 2004; Burt et al., 1997; Cacciapuoti et al., 2003; Hellweg et al., 2003; Regal et al., 2004b) but those methods are still very difficult to realize experimentally. While the measurement of higher-order correlations is challenging already for bosons, the theory of these correlations has been established a long time ago by Glauber for photons (Glauber, 1963a,b; Naraschewski and Glauber, 1999). For fermions however, despite some efforts (Cahill and Glauber, 1999) a satisfactory coherence *theory* is still missing.

From the previous section we know that one can circumvent these difficulties by making use of the nonlinear coupling of atoms to a molecular field. The nonlinearity of the coupling links first-order correlations of the molecules to second-order correlations of the atoms. Furthermore the molecules are always bosonic so that the well-known coherence theory for bosonic fields can be used to characterize them. Considering a simplified model with only one molecular mode, it was found that the molecules created that way can indeed be used as a diagnostic tool for second-order correlations of the original atomic field.

We consider the limiting case of strong atom-molecule coupling as compared to the relevant atomic energies. The molecule formation from a Bose-Einstein condensate (BEC) serves as a reference system. There we can rather easily study the contributions to the molecular signal from the condensed fraction as well as from thermal and quantum fluctuations above the condensate. The cases of a normal Fermi gas and a BCS superfluid Fermi system are then compared with it. We show that the molecule formation from a normal Fermi gas and from the unpaired fraction of atoms in a BCS state has very similar properties to those of the molecule formation from the non-condensed atoms in the BEC case. The state of the molecular field formed from the pairing field in the BCS state on the other hand is similar to that resulting from the condensed fraction in the BEC case. The qualitative information gained by the analogies with the BEC case help us gain a physical understanding of the molecule formation in the BCS case where direct calculations are difficult and not nearly as transparent.

### A. Model

We consider again the three cases where the atoms are bosonic and initially form a BEC, or consist of two species of ultra-cold fermions (labeled again by  $\sigma = \uparrow, \downarrow$ ), with or without superfluid component. In the following we describe explicitly the situation for fermions, the bosonic case being obtained from it by omitting the spin indices and by

replacing the Fermi field operators by bosonic field operators.

Since we are primarily interested in how much can be learned about the second-order correlations of the initial atomic cloud from the final molecular state, we keep the physics of the atoms themselves as well as the coupling to the molecular field as simple as possible. The coupled fermion-molecule system can be described by the Hamiltonian (Chiofalo et al., 2002; Holland et al., 2001; Timmermans et al., 1999)

$$\begin{aligned} \hat{H} = & \sum_{\mathbf{k}, \sigma} \frac{\omega_{\mathbf{k}}}{2} \hat{c}_{\mathbf{k}\sigma}^\dagger \hat{c}_{\mathbf{k}\sigma} + \sum_{\mathbf{k}} \omega_{\mathbf{k}} \hat{a}_{\mathbf{k}}^\dagger \hat{a}_{\mathbf{k}} + V^{-1/2} \sum_{\mathbf{k}_1, \mathbf{k}_2, \sigma} \tilde{U}_{\text{tr}}(\mathbf{k}_2 - \mathbf{k}_1) \hat{c}_{\mathbf{k}_2\sigma}^\dagger \hat{c}_{\mathbf{k}_1\sigma} \\ & + \frac{U_0}{2V} \sum_{\mathbf{q}, \mathbf{k}_1, \mathbf{k}_2} \hat{c}_{\mathbf{k}_1+\mathbf{q}\uparrow}^\dagger \hat{c}_{\mathbf{k}_2-\mathbf{q}\downarrow}^\dagger \hat{c}_{\mathbf{k}_2\downarrow} \hat{c}_{\mathbf{k}_1\uparrow} + \hbar g \left( \sum_{\mathbf{q}, \mathbf{k}} \hat{a}_{\mathbf{q}}^\dagger \hat{c}_{\mathbf{q}/2+\mathbf{k}\downarrow} \hat{c}_{\mathbf{q}/2-\mathbf{k}\uparrow} + \text{H.c.} \right) \end{aligned} \quad (40)$$

The kinetic energies  $\omega_{\mathbf{k}}$  are defined as before,  $V$  is the quantization volume,  $\tilde{U}_{\text{tr}}(\mathbf{k}) = V^{-1/2} \int_V d^3x e^{-i\mathbf{k}\mathbf{x}} U_{\text{tr}}(\mathbf{x})$  is the Fourier transform of the trapping potential  $U_{\text{tr}}(\mathbf{r})$  and  $U_0 = 4\pi\hbar^2 a/m_f$  is the background scattering strength with  $a$  the background scattering length. The coupling constant  $g$  between atoms and molecules is, up to dimensions, equal to  $\chi$  of the previous sections.

We assume that the trapping potential and background scattering are relevant only for the preparation of the initial state before the coupling to the molecules is switched on at  $t = 0$  and can be neglected in the calculation of the subsequent dynamics. This is justified if  $\hbar g\sqrt{N} \gg U_0 n, \hbar\omega_i$  where  $n$  is the atomic density,  $N$  the number of atoms, and  $\omega_i$  are the oscillator frequencies of the atoms in the potential  $U_{\text{tr}}(\mathbf{r})$  that is assumed to be harmonic. Experimentally, the interaction between the atoms can effectively be switched off by ramping the magnetic field to a position where the scattering length is zero, so that this assumption is fulfilled.

Regarding the strength of the coupling constant  $g$ , two cases are possible:  $\hbar g\sqrt{N}$  can be much larger or much smaller than the characteristic kinetic energies involved. For fermions the terms broad and narrow resonance have been coined for the two cases, respectively, and we will use these for bosons as well. Both situations can be realized experimentally, and they give rise to different effects. For strong coupling the conversion process needs not satisfy energy conservation because of the energy time uncertainty relation. For weak coupling energy conservation is enforced. This energy selectivity can be useful in certain situations because it allows one to resolve additional structures in the atomic state. The analysis of this case is fairly technical, however. Therefore we only consider the case of strong coupling and refer the interested reader to (Meiser et al., 2005b) for details of the calculations and the case of weak coupling.

First-order time-dependent perturbation theory requires that the state of the atoms does not change significantly and consequently, only a small fraction of the atoms are converted into molecules. It is reasonable to assume that

this is true for short interaction times or weak enough coupling. Apart from making the system tractable by analytic methods there is also a deeper reason why the coupling should be weak: Since we ultimately wish to get information about the atomic state, it should not be modified too much by the measurement itself, i.e. the coupling to the molecular field. Our treatment therefore follows the same spirit as Glauber's original theory of photon detection, where it is assumed that the light-matter coupling is weak enough that the detector photocurrent can be calculated using Fermi's Golden rule.

## B. BEC

We consider first the case where the initial atomic state is a BEC in a spherically symmetric harmonic trap. We assume that the temperature is well below the BEC transition temperature and that the interactions between the atoms are not too strong. Then the atomic system is described by the field operator

$$\hat{\psi}(\mathbf{x}) = \psi_0(\mathbf{x})\hat{c} + \delta\hat{\psi}(\mathbf{x}), \quad (41)$$

where  $\psi_0(\mathbf{x})$  is the condensate wave function and  $\hat{c}$  is the annihilation operator for an atom in the condensate. In accordance with the assumption of low temperatures and weak interactions we do not distinguish between the total number of atoms and the number of atoms in the condensate. The fluctuations  $\delta\hat{\psi}(\mathbf{x})$  are small and those with wavelengths much less than  $R_{TF}$  will be treated in the local density approximation while those with wavelengths comparable to  $R_{TF}$  can be neglected (Bergeman et al., 2000; D. A. W. Hutchinson and Zaremba, 1997; Reidl et al., 1999).

We are interested in the momentum distribution of the molecules

$$n(\mathbf{p}, t) = \langle \hat{b}_{\mathbf{p}}^\dagger(t) \hat{b}_{\mathbf{p}}(t) \rangle \quad (42)$$

which for short times,  $t$ , can be calculated using perturbation theory. In the broad resonance limit we ignore the kinetic energies and find

$$n_{\text{BEC}}(\mathbf{p}, t) = (gt)^2 N(N-1)V \left| \tilde{\psi}_0^2(\mathbf{p}) \right|^2 + (gt)^2 4N \int \frac{d^3x}{V} \langle \delta\hat{c}_{\mathbf{p}}^\dagger(\mathbf{x}) \delta\hat{c}_{\mathbf{p}}(\mathbf{x}) \rangle, \quad (43)$$

where the expectation value in the last term includes a thermal average. From this expression we see that our approach is justified if  $(\sqrt{N}gt)^2 \ll 1$  because for such times the initial atomic state can be assumed to remain undepleted. The first term in Eq. (43) is the contribution from condensed atoms and the second term comes from uncondensed atoms

above the condensate. The contribution from the condensate can be evaluated in closed form in the Thomas Fermi approximation for a spherical trap. The contribution from the thermal atoms can be calculated using the local density approximation. The details of this calculation can be found in Ref. (Meiser et al., 2005b).

The momentum distribution (43) is illustrated in Fig. 13. The contribution from the condensate is a collective effect, as indicated by its quadratic scaling with the atom number. It clearly dominates over the incoherent contribution from the fluctuations, which is proportional to the number of atoms and only visible in the inset. The momentum width of the contribution from the condensate is roughly  $\hbar 2\pi/R_{TF}$  which is much narrower than the contribution from the fluctuations, whose momentum distribution has a typical width of  $\hbar/\xi$ , where  $\xi = (8\pi an)^{-1/2}$  is the healing length. This is a case where coherence properties of the atoms can be read off the momentum distribution of the molecules: The narrow momentum distribution of the molecules is only possible if the atoms were coherent over distances  $\sim R_{TF}$ . At this point this is a fairly trivial observation and the same information could have been gained by looking directly at the momentum distribution of the atoms, which is after all how Bose-Einstein condensation was detected already in the very first experiments (Anderson et al., 1995; Bradley et al., 1995; Davis et al., 1995). Still we mention it because it will be very interesting (indeed interesting enough to motivate this whole work!) to contrast this situation to the BCS case below.

Using the same approximation scheme we can calculate the second-order correlation. If we neglect fluctuations we find

$$g_{\text{BEC}}^{(2)}(\mathbf{p}_1, t_1; \mathbf{p}_2, t_2) = 1 - \frac{6}{N} + \mathcal{O}(N^{-2}). \quad (44)$$

For  $N \rightarrow \infty$  this is very close to 1, which is characteristic of a coherent state. This result implies that the number fluctuations of the molecules are very nearly Poissonian. The fluctuations lead to a larger value of  $g^{(2)}$ , making the molecular field partially coherent, but their effect is only of order  $\mathcal{O}(N^{-1})$ .

### C. Normal Fermi gas

We treat the gas in the local density approximation where the atoms locally fill a Fermi sea

$$|NFG\rangle = \prod_{|\mathbf{k}| < k_F(\mathbf{x})} \hat{c}_{\mathbf{k}}^\dagger |0\rangle \quad (45)$$

with local Fermi momentum  $\hbar k_F(\mathbf{x})$  and  $|0\rangle$  being the atomic vacuum. It is related to the local density of the atoms in the usual way (D. A. Butts and D. S. Rokhsar, 1997; Landau et al., 1980).

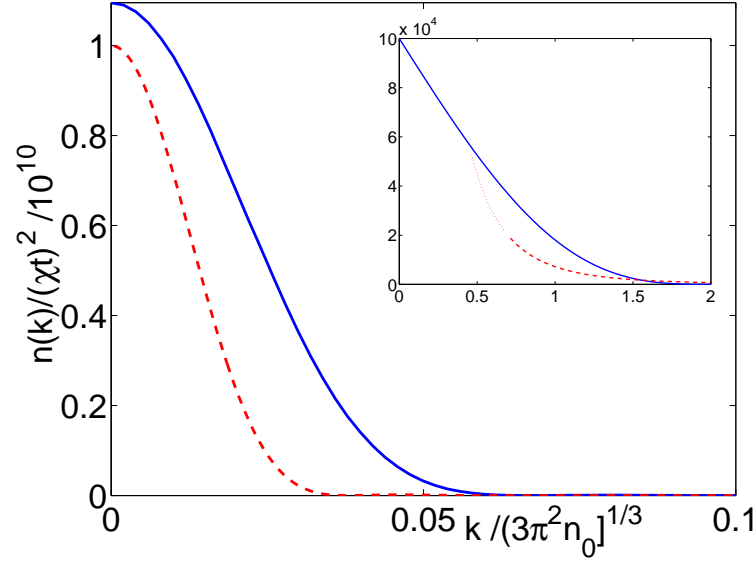


FIG. 13 Momentum distribution of molecules formed from a BEC (red dashed line) with  $a = 0.1a_{\text{osc}}$  and  $T = 0.1T_c$  and a BCS type state with  $k_F a = 0.5$  and  $a_{\text{osc}} = 5k_F^{-1}(0)$  (blue solid line), both for  $N = 10^5$  atoms. The BCS curve has been scaled up by a factor of 20 for easier comparison. The inset shows the noise contribution for BEC (red dashed) and BCS (blue) case. The latter is simply the momentum distribution of molecules formed from a normal Fermi gas. The local density approximation treatment of the noise contribution in the BEC case is not valid for momenta smaller than  $2\pi/\xi$  (indicated by the red dotted line in the inset). Note that the coherent contribution is larger than the noise contribution by five orders of magnitude in the BEC case and three orders of magnitude in the BCS case.

The momentum distribution and second order correlation function are readily found in perturbation theory. The momentum distribution is shown in the inset in Fig. 13. The total number of molecules scales only linear with the number of atoms, meaning that, in contrast to the BEC case, the molecule formation is non-collective. Each atom pair is converted into a molecule independently of all the others and there is no collective enhancement. Furthermore the momentum distribution of the atoms is much wider than in the BEC case. It's width is of the order of  $\hbar n_0^{1/3}$  indicating that the atoms are correlated only over distances comparable to the inter atomic distance.

Similarly, we find for the local value of  $g^{(2)}$  at position  $\mathbf{x}$

$$\begin{aligned} g_{\text{loc}}^{(2)}(\mathbf{p}, \mathbf{x}, t) &\equiv g_{\text{loc}}^{(2)}(\mathbf{p}, t; \mathbf{p}, t, \mathbf{x}) \\ &= 2 \left( 1 - \frac{1}{N_{\text{eff}}(\mathbf{p}, \mathbf{x})} \right), \end{aligned} \quad (46)$$

where  $N_{\text{eff}}$  is the number of atoms that are allowed to form a molecule on the basis of momentum conservation. For large  $N_{\text{eff}}$   $g^{(2)}$  approaches 2 which is characteristic of a thermal field. Indeed, using the analogy with an ensemble of two level atoms coupled to every mode of the molecular field provided by the Tavis-Cummings model, it is easy to

see that the entire counting statistics is thermal.

#### D. BCS state

Let us finally consider a system of fermions with attractive interactions,  $U_0 < 0$ , at temperatures well below the BCS critical temperature. As is well known, for these temperatures the attractive interactions give rise to correlations between pairs of atoms in time reversed states known as Cooper pairs. We assume that the spherically symmetric trapping potential is sufficiently slowly varying that the gas can be treated in the local density approximation. More quantitatively, the local density approximation is valid if the size of the Cooper pairs, given by the correlation length

$$\lambda(r) = v_F(r)/\pi\Delta(r),$$

is much smaller than the oscillator length for the trap. Here,  $v_F(r)$  is the velocity of atoms at the Fermi surface and  $\Delta(r)$  is the pairing field at distance  $r$  from the origin, which we take at the center of the trap. Loosely speaking, in the local density approximation the ground state of the atoms is determined by repeating the variational BCS-calculation of the previous section in a small volume at every position  $\mathbf{x}$ . A thorough discussion of this calculation can be found in Ref. (Houbiers et al., 1997).

We find the momentum distribution of the molecules from the BCS-type state by repeating the calculation done in the case of a normal Fermi gas. For the BCS wave function, the relevant atomic expectation values factorize into normal and anomalous correlations. The normal terms are proportional to densities and are already present in the case of a normal Fermi gas while the anomalous contributions are proportional to the gap parameter. The momentum distribution of the molecules becomes

$$n_{\text{BCS}}(\mathbf{p}, t) \approx (gt)^2 \left| \sum_k \langle \hat{c}_{\mathbf{p}/2+\mathbf{k},\downarrow} \hat{c}_{\mathbf{p}/2-\mathbf{k},\uparrow} \rangle \right|^2 + n_{\text{NFG}}(\mathbf{p}, t). \quad (47)$$

The first term is easily shown to be proportional to the square of the Fourier transform of the gap parameter. Since the gap parameter is slowly varying over the size of the atomic cloud, this contribution has a width of the order of  $\hbar/R_{TF}$ , in complete analogy with the BEC case above. The total number of atoms in the first contribution is proportional to the square of the number of Cooper pairs, which is a macroscopic fraction of the total atom number well below the BCS transition temperature. That means that this contribution is a collective effect. The second term is the wide and incoherent non-collective contribution already present in the case of a normal Fermi gas. It is very similar to the thermal noise in the BEC case as far as its coherence properties are concerned.

For weak interactions such that the coherent contribution is small compared to the incoherent contribution, the second order correlations are close to those of a normal Fermi gas given by Eq. (46),  $g^{(2)}(\mathbf{p}, \mathbf{x}, t) \approx 2$ . However, in the strongly interacting regime,  $k_F|a| \sim 1$ , and large  $N$ , the coherent contribution from the paired atoms dominates over the incoherent contribution from unpaired atoms. In this limit one finds that the second-order correlation is close to that of the BEC,  $g^{(2)}(\mathbf{p}, \mathbf{x}, t) \approx 1$ . The physical reason for this is that at the level of even order correlations the pairing field behaves just like the mean field of the condensate. This is clear from the factorization property of the atomic correlation functions in terms of the normal component of the density and the anomalous density contribution due to the mean field. In this case, the leading order terms in  $N$  are given by the anomalous averages.

To summarize, molecules produced from an atomic BEC show a rather narrow momentum distribution that is comparable to the zero-point momentum width of the BEC from which they are formed. The molecule production is a collective effect with contributions from all atom pairs adding up constructively, as indicated by the quadratic scaling of the number of molecules with the number of atoms. Each mode of the resulting molecular field is to a very good approximation coherent (up to terms of order  $\mathcal{O}(1/N)$ ). The effects of noise, both due to finite temperatures and to vacuum fluctuations, are of relative order  $\mathcal{O}(1/N)$ . They slightly increase the  $g^{(2)}$  and cause the molecular field in each momentum state to be only partially coherent.

In contrast, the momentum distribution of molecules formed from a normal Fermi gas is much broader with a typical width given by the Fermi momentum of the initial atomic cloud, i.e. the atoms are only correlated over an interatomic distance. The molecule production is not collective as the number of molecules only scales like the number of atoms rather than the square. In this case, the second-order correlations of the molecules exhibit super-Poissonian fluctuations, and the molecules are well characterized by a thermal field.

The case where molecules are produced from paired atoms in a BCS-like state shares many properties with the BEC case: The molecule formation rate is collective, their momentum distribution is very narrow, corresponding to a coherence length of order  $R_{TF}$ , and the molecular field is essentially coherent. The non-collective contribution from unpaired atoms has a momentum distribution very similar to that of the thermal fluctuations in the BEC case.

## VI. CONCLUSION

In this paper we have used three examples to illustrate the profound impact of quantum optics paradigms, tools and techniques, on the study of low-density, quantum-degenerate atomic and molecular systems. There is little doubt that the remarkably fast progress witnessed by that field results in no little part from the experimental and theoretical

methods developed in quantum optics over the last decades. It is therefore fitting, on the occasion of Herbert Walther's seventieth birthday, to reflect on the profound impact of the field that he has helped invent, and where he has been and remains so influential, on some of the most exciting developments in AMO science.

### Acknowledgments

This work was supported in part by the US Office of Naval Research, by the National Science Foundation, by the US Army Research Office, and by the National Aeronautics and Space Administration.

### References

- Altman, E., Demler, E., Lukin, M. D., July 2004. Probing many-body states of ultracold atoms via noise correlations. *Phys. Rev. A* 70, 013603.
- Anderson, M. H., Ensher, J. R., Mathews, M. R., Wieman, C. E., Cornell, E. E., 1995. Observation of bose-einstein condensation in a dilute atomic vapor. *Science* 269, 198.
- Anderson, P. W., 1958. Random-phase approximation in the theory of superconductivity. *Phys. Rev.* 112, 1900.
- Andreev, A. V., Gurarie, V., Radzihovsky, L., 2004. Nonequilibrium dynamics and thermodynamics of a degenerate fermi gas across a feshbach resonance. *Phys. Rev. Lett.* 93, 130402.
- Andrews, M. R., Townsend, C. G., H.-J. Miesner, Durfee, D. S., Kurn, D. M., Ketterle, W., 1997. Observation of interference between two bose condensates. *Science* 275, 637–641.
- Anglin, J. R., Vardi, A., 2001. Dynamics of two-mode bose-einstein condensate beyond mean field. *Phys. Rev. A* 64, 013605.
- Bach, R., Rzażewski, K., May 2004. Correlations in atomic systems: Diagnosing coherent superpositions. *Phys. Rev. Lett.* 92 (20), 200401.
- Barankov, R. A., Levitov, L. S., September 2004. Atom-molecule coexistence and collective dynamics near a feshbach resonance of cold fermions. *Phys. Rev. Lett.* 93 (13), 130403.
- Barnett, S. M., Pegg, D. T., 1990. Quantum theory of optical phase correlations. *Phys. Rev. A* 42, 6713.
- Bartenstein, M., Altmeyer, A., Riedl, S., Jochim, S., Chin, C., J. Hecker Denschlag, Grimm, R., 2004. Collective excitations of a degenerate gas at the bec-bcs crossover. *Phys. Rev. Lett.* 92, 203201.
- Bergeman, T., Feder, D. L., Balazs, N. L., Schneider, B. I., 2000. Bose condensates in a harmonic trap near the critical temperature. *Phys. Rev. A* 61, 063605.
- Bradley, C. C., Sackett, C. A., Tollett, J. J., Hulet, R. G., 1995. Evidence of bose-einstein condensation in an atomic gas with attractive interactions. *Phys. Rev. Lett.* 75, 1687.

- Brattke, S., B. T. H. Varcoe, Walther, H., 2001. Generation of photon number states on demand via cavity quantum electrodynamics. *Phys. Rev. Lett.* 86, 3534.
- Burgbacher, F., Audretsch, J., November 1999. Beam splitter for bose-einstein condensates based on bragg scattering from a cavity mode. *Phys. Rev. A* 60 (5), 3385.
- Burt, E. A., Christ, R. W., Myatt, C. J., Holland, M. J., Cornell, E. A., Wieman, C. E., July 1997. Coherence, correlations, and collisions: What one learns about bose-einstein condensates from their decay. *Phys. Rev. Lett.* 79 (3), 337.
- Cacciapuoti, L., Hellweg, D., Kottke, M., Schulte, T., Ertmer, W., Arlt, J. J., November 2003. Second-order correlation function of a phase fluctuating bose-einstein condensate. *Phys. Rev. A* 68, 053612.
- Cahill, K. E., Glauber, R. J., February 1999. Density operators for fermions. *Phys. Rev. A* 59 (2), 1538.
- Chin, C., Bartenstein, M., Altmeyer, A., Riedl, S., Jochim, S., J. Hecker Denschlag, Grimm, R., 2004. Observation of the pairing gap in a strongly interacting fermi gas. *Science* 305, 1128.
- Chiofalo, M. L., Kokkelmans, S. J. J. M. F., Milstein, J. N., Holland, M. J., 2002. Signatures of resonance superfluidity in a quantum fermi gas. *Phys. Rev. Lett.* 88 (9), 090402.
- Christ, H., Search, C. P., Meystre, P., 2003. Dynamics of fermionic four-wave mixing. *Phys. Rev. A* 67, 063611.
- D. A. Butts, D. S. Rokhsar, 1997. Trapped fermi gases. *Phys. Rev. A* 55, 4346.
- D. A. W. Hutchinson, Zaremba, E., 1997. Finite temperature excitations of a trapped bose gas. *Phys. Rev. Lett.* 78 (10), 1842.
- Damski, B., Santos, L., Tiemann, E., Lewenstein, M., Kotochigova, S., Julienne, P., Zoller, P., 2003. Creation of a dipolar superfluid in optical lattices. *Phys. Rev. Lett.* 90, 110401.
- Davis, K., Mewes, M. O., Andrews, M. R., van Druten, N. J., Durfee, D. S., Kurn, D. M., Ketterle, W., 1995. Bose-einstein condensation in a gas of sodium atoms. *Phys. Rev. Lett.* 75, 3969.
- DeMarco, B., Jin, D. S., 1998. Exploring a quantum degenerate gas of fermionic atoms. *Phys. Rev. A* 58, R4267.
- DeMarco, B., Jin, D. S., 1999. Onset of fermi degeneracy in a trapped atomic gas. *Science* 285, 1703.
- Donley, E. A., Claussen, N. R., Thompson, S. T., Wieman, C. E., 2002. Atom-molecule coherence in a bose-einstein condensate. *Nature (London)* 417, 529.
- Duine, D. A., Stoof, H. T. C., 2004. Atom-molecule coherence in bose gases. *Phys. Rep.* 396, 115–195.
- Dürr, S., Volz, T., Marte, A., Rempe, G., 2004. Observation of molecules produced from a bose-einstein condensate. *Phys. Rev. Lett.* 92, 020406.
- Esslinger, T., Molmer, K., 2003. Atoms and molecules in lattices : Bose-einstein condensates built on a shared vacuum. *Phys. Rev. Lett.* 90, 160406.
- Filipowicz, P., Javanainen, J., Meystre, P., 1986. Theory of a microscopic maser. *Phys. Rev. A* 34, 3077.
- Fisher, M. P., Weichman, P. B., Grinstein, G., Fisher, D. S., 1989. Boson localization and the superfluid-insulator transition. *Phys. Rev. B* 40, 546.

- Glauber, R. J., September 1963a. Coherent and incoherent states of the radiation field. *Phys. Rev.* 131 (6), 2766.
- Glauber, R. J., June 1963b. The quantum theory of optical coherence. *Phys. Rev.* 130 (6), 2529.
- Greiner, M., Mandel, O., Esslinger, T., Hänsch, T. W., Bloch, I., January 2002a. Quantum phase transition from a superfluid to a mott insulator in a gas of ultracold atoms. *Nature (London)* 415, 39.
- Greiner, M., Mandel, O., Hänsch, T. W., Bloch, I., September 2002b. Collapse and revival of the matter wave field of a bose-einstein condensate. *Nature (London)* 419, 51.
- Greiner, M., Regal, C. A., Jin, D. S., 2003. Emergence of a molecular bose-einstein condensate from a fermi gas. *Nature (London)* 426, 537.
- Guzman, A. M., Meystre, P., Wright, E. M., 1989. Semiclassical theory of a micromaser. *Phys. Rev. A* 40, 2471.
- Hadzibabic, Z., Gupta, S., Stan, C. A., Schunck, C. H., Zwierlein, M. W., Dieckmann, K., Ketterle, W., 2003. Fiftyfold improvement in the number of quantum degenerate fermionic atoms. *Phys. Rev. Lett.* 91, 160401.
- Heinzen, D. J., Wynar, R., Drummond, P. D., Kheruntsyan, 2000. Superchemistry: Dynamics of coupled atomic and molecular bose-einstein condensates. *Phys. Rev. Lett.* 84, 5029.
- Hellweg, D., Cacciapuoti, L., Kottke, M., Schulte, T., Sengstock, K., Ertmer, W., Arlt, J. J., July 2003. Measurement of the spatial correlation function of phase fluctuating bose-einstein condensates. *Phys. Rev. Lett.* 91 (1), 010406.
- Holland, M., Kokkelmans, S. J. J. M. F., Chiofalo, M. L., Walser, R., 2001. Resonance superfluidity in a quantum degenerate fermi gas. *Phys. Rev. Lett.* 87, 120406.
- Houbiers, M., Ferwerda, R., Stoof, H. T. C., McAlexander, W. I., Sackett, C. A., Hulet, R. G., December 1997. Superfluid state of atomic  ${}^6\text{Li}$  in a magnetic trap. *Phys. Rev. A* 56 (6), 4864.
- Inouye, S., Andrews, M. R., Stenger, J., Miesner, H.-J., Stamper-Kurn, D. M., Ketterle, W., 1998. Observation of feshbach resonances in a bose-einstein condensate. *Nature (London)* 392, 151.
- Inouye, S., Chikkatur, A. P., Stamper-Kurn, D. M., Stenger, J., Ketterle, W., 1999a. Superradiant rayleigh scattering from a bose-einstein condensate. *Science* 285, 571.
- Inouye, S., Goldwin, J., Olsen, M. L., Ticknor, C., Bohn, J. L., Jin, D. S., 2004. Observation of heteronuclear feshbach resonances in a mixture of bosons and fermions. *Phys. Rev. Lett.* 93, 183201.
- Inouye, S., Pfau, T., Gupta, S., Chikkatur, A. P., Görlitz, A., Pritchard, D. E., Ketterle, W., 1999b. Phase-coherent amplification of atomic matter waves. *Nature (London)* 402, 641.
- Jaksch, D., Bruder, C., Cirac, J. I., Zoller, P., October 1998. Cold bosonic atoms in optical lattices. *Phys. Rev. A* 81 (15), 3108.
- Jaksch, D., Venturi, V., Cirac, J. I., Williams, C. J., Zoller, P., 2002. Creation of a molecular condensate by dynamically melting a mott insulator. *PRL* 89, 040402.
- Jaksch, D., Zoller, P., 2005. The cold atom hubbard toolbox. *Ann. Phys.* 315, 52–79.
- Javanainen, J., Ivanov, M. Y., 1999. Splitting a trap containing a bose-einstein condensate: Atom number fluctuations. *Phys.*

- Rev. A 60, 2351.
- Javanainen, J., Kostrun, M., Zheng, Y., Carmichael, A., Shrestha, U., Meinel, P. J., Mackie, M., Dannenberg, O., Suominen, K.-A., May 2004. Collective molecule formation in a degenerate fermi gas via a feshbach resonance. Phys. Rev. Lett. 92, 200402.
- Javanainen, J., Mackie, M., May 1999. Coherent photoassociation of a bose-einstein condensate. Phys. Rev. A 59 (5), R3186.
- Jochim, S., Bartenstein, M., Altmeyer, A., Hendl, G., Riedl, S., Chin, C., Denschlag, J. H., Grimm, R., 2003. Bose-einstein condensation of molecules. Science 302, 2101.
- Kerman, A. J., Sage, J. M., Sainis, S., Bergeman, T., DeMille, D., 2004. Production of ultracold, polar rbc<sup>s\*</sup> molecules via photoassociation. Phys. Rev. Lett. 92, 033004.
- Ketterle, W., H.-J. Miesner, 1997. Coherence properties of bose-einstein condensates and atom lasers. Phys. Rev. A 56, 3291–3293.
- Kinast, J., S. L. Hemmer, Gehm, M., Turlapov, A., J. E. Thomas, 2004. Evidence for superfluidity in a resonantly interacting fermi gas. Phys. Rev. Lett. 92, 150402.
- Kittel, C., 1987. Quantum theory of solids, 2nd Edition. John Wiley & Sons.
- Kohl, M., Moritz, H., Stoferle, T., Gunter, K., Esslinger, T., 2005. Fermionic atoms in a three dimensional optical lattice : Observing fermi surfaces, dynamics, and intereactios. Phys. Rev. Lett. 94, 080403.
- Kozierowski, M., R. Tanaś, May 1977. Quantum fluctuations in second-harmonic light generation. Opt. Commun. 21 (2), 229.
- Kozuma, M., Suzuki, Y., Torii, Y., Sigiura, T., Kuga, T., Hagley, E. E., Deng, L., 1999. Phase-coherent amplification of matter wave. Science 286, 2309.
- Krause, J., Scully, M. O., Walther, T., Walther, H., 1989. Preparation of a pure number state and measurement of the photon statistics in a high-q micromaser. Phys. Rev. A 39, 1915.
- Landau, L. D., Lifshitz, E. M., Pitaevski, L. P., 1980. Statistical Physics, Part 2, 3rd Edition. Butterworth-Heinemann.
- Law, C. K., Bigelow, N. P., December 1998. Amplifying an atomic wave signal using a bose-einstein condensate. Phys. Rev. A 58 (6), 4791.
- Leggett, A. J., 2001. Bose-einstein condensation in the alkali gases : Some fundamental concepts. Review of Modern Physics 73, 307.
- Lenz, G., Lax, P., Meystre, P., August 1993. Exchange force in the near-resonant kapitza-dirac effect. Phys. Rev. A 48 (2), 1707.
- Luis, A., Sanchez-Soto, L. L., 1993. Phase-difference operator. Phys. Rev. A 48, 4702.
- Mandel, L., August 1982. Squeezing and photon antibunching in harmonic generation. Opt. Commun. 42 (6), 437.
- Mandel, O., Greiner, M., Widera, A., RÖm, T., Hansch, T. W., Bloch, I., 2004. Coherent transport of neutral atoms in spin-dpendent optical lattice potentials. Phys. Rev. Lett. 91, 010407.

- Meiser, D., Meystre, P., 2005. Number statistics of molecules formed by ultra-cold atoms. *Phys. Rev. Lett.* 94, 093001.
- Meiser, D., Search, C. P., Meystre, P., 2005a. Diffraction of ultracold fermions by quantized light fields: Standing versus traveling waves. *Phys. Rev. A* 71, 013404.
- Meiser, D., Search, C. P., Meystre, P., 2005b. Molecule formation as a diagnostic tool for second order correlations of ultra-cold gases. *Phys. Rev. A* 71, 033621.
- Meschede, D., Walther, H., Muller, G., 1985. One-atom maser. *Phys. Rev. Lett.* 54, 551.
- Meystre, P., III, M. S., 1999. "Elements of Quantum Optics", 3rd Edition. Springer-Verlag.
- Miyakawa, T., Christ, H., Search, C. P., Meystre, P., 2003. Four-wave mixing in degenerate fermi gases: Beyond the undepleted pump approximation. *Phys. Rev. A* 67, 063603.
- Miyakawa, T., Meystre, P., 2005. Boson-fermion coherence in a spherically symmetric harmonic trap. *Phys. Rev. A* 71, 033624.
- Miyakawa, T., Search, C. P., Meystre, P., 2004. Phase coherence in a driven double-well system. *Phys. Rev. A* 70, 053622.
- Molmer, K., 2003. Jaynes-cummings dynamics with a matter wave oscillator. *Phys. Rev. Lett.* 90.
- Moore, M., Zobay, O., Meystre, P., August 1999. Quantum optics of a bose-einstein condensate coupled to a quantized light field. *Phys. Rev. A* 60 (2), 1491.
- Moore, M. G., Meystre, P., 1999. Theory of superradiant scattering of laser light from bose-einstein condensates. *Phys. Rev. Lett.* 83, 5202.
- Moore, M. G., Sadeghpour, H. R., 2003. Controlling two-species mott-insulator phases in an optical lattice to form an array of dipolar molecules. *Phys. Rev. A* 67, 041603.
- Naraschewski, M., Glauber, R. J., June 1999. Spatial coherence and density correlations of trapped bose gases. *Phys. Rev. A* 59 (6), 4595.
- Ohashi, Y., Griffin, A., 2002. Bcs-bec crossover in a gas of fermi atoms with a feshbach resonance. *Phys. Rev. Lett.* 89, 130402.
- Pegg, D. T., Barnett, S. M., 1988. Unitary phase operator in quantum mechanics. *Europhysics Letters* 6, 483.
- Regal, C. A., Greiner, M., Jin, D. S., January 2004a. Observation of resonance condensation of fermionic atom pairs. *Phys. Rev. Lett.* 92 (4), 040403.
- Regal, C. A., Greiner, M., Jin, D. S., 2004b. Observation of resonance condensation of fermionic atom pairs. *Phys. Rev. Lett.* 92, 040403.
- Regal, C. A., Ticknor, C., Bohn, J. L., Jin, D. S., 2003. Creation of ultracold molecules from a fermi gas of atoms. *Nature (London)* 424, 47.
- Reidl, J., Csordás, A., Graham, R., Szépfalussy, P., 1999. Finite-temperature excitations of bose gases in anisotropic traps. *Phys. Rev. A* 59 (5), 3816.
- Remoe, G., Schmidt-Kaler, F., Walther, H., 1990. Observation of sub-poissonian photon statistics in a micromaser. *Phys. Rev. Lett.* 64, 2783.

- Rempe, G., Schmidt-Kaler, F., Walther, H., 1990. Observation of sub-poissonian photon statistics in a micromaser. *Phys. Rev. Lett.* 64, 2783.
- Rempe, G., Walther, H., 1990. Sub-poissonian atomic statistics in a micromaser. *Phys. Rev. A* 42, 1650.
- Rojo, A., Cohen, J., Berman, P., 1999. Talbot oscillations and periodic focusing in a one-dimensional condensate. *Phys. Rev. A* 60, 1482.
- Rom, T., Best, T., Mandel, O., Widera, A., Greiner, M., Hansch, T., Bloch, I., 2004. State selective production of molecules in optical lattices. *Phys. Rev. Lett.* 93, 073002.
- Ryu, C., Du, X., Dudarev, A. M., Wan, S., Niu, Q., Heinzen, D. J., 2005. Raman-induced oscillation between an atomic and molecular quantum gas .
- Scully, M. O., Zubairy, M. S., 1997. *Quantum Optics*. Cambridge University Press.
- Search, C. P., Miyakawa, T., Meystre, P., 2004. A lattice array of molecular micromasers. *Optics Express* 12, 30.
- Search, C. P., Potting, S., Zhang, W., Meystre, P., 2002a. Input-output theory for fermions in an atom cavity. *Phys. Rev. A* 66, 043616.
- Search, C. P., Pu, H., Zhang, W., Meystre, P., March 2002b. Diffraction of a superfluid fermi gas by an atomic grating. *Phys. Rev. Lett.* 88 (11), 110401.
- Search, C. P., Zhang, W., Meystre, P., 2003. Molecular micromaser. *Phys. Rev. Lett.* 91, 190401.
- Stan, C. A., Zwiernik, M. W., Schunck, C. H., Raupach, S. M. F., Ketterle, W., October 2004. Observation of feshbach resonances between two different atomic species. *Phys. Rev. Lett.* 93 (14), 143001.
- Stoferle, T., Moritz, H., Gunter, K., Kohl, M., Esslinger, T., 2005. Molecules of fermionic atoms in an optical lattice .
- Tavis, M., Cummings, F. W., June 1968. Exact solution for an n-molecule-radiation-field hamiltonian. *Phys. Rev.* 170, 379.
- Theis, M., Thalhammer, G., Winkler, K., Hellwig, M., Ruff, G., Grimm, R., 2004. Tuning the scattering length with an optically induced feshbach resonance. *Phys. Rev. Lett.* 93, 123001.
- Tikhonenkov, I., Vardi, A., 2004 .
- Timmermans, E., Furuya, K., Milonni, P. W., Kerman, A. K., 2001. Prospect of creating a composite fermi-bose superfluid. *Phys. Lett. A* 285, 228.
- Timmermans, E., Tommasini, P., Hussein, M., Kerman, A., 1999. Feshbach resonances in atomic bose-einstein condensates. *Phys. Rep.* 315, 199–230.
- Uys, H., Miyakawa, T., Meiser, D., Meystre, P., 2005. Fluctuations in the formation time of ultracold dimers from fermionic atoms .
- Walther, H., 1992. Experiments on cavity quantum electrodynamics. *Physics reports* 219, 263.
- Wynar, R., R. S. Freeland, D. J. H., Ryu, C., Heinzen, D. J., 2000. Molecules in a bose-einstein condensate. *Science* 287, 1016.
- Zwiernik, M. W., Abo-Shaeer, J. R., Schirotzek, A., Schunck, C. H., Ketterle, W., 2005. Vortices and superfluidity in a strongly

interacting fermi gas. *Nature*, London 435, 1047.

Zwierlein, M. W., Stan, C. A., Schunck, C. H., Kerman, A. J., Ketterle, W., 2004. Condensation of pairs of fermionic atoms near a feshbach resonance. *Phys. Rev. Lett.* 93, 120403.

Zwierlein, M. W., Stan, C. A., Schunck, C. H., Raupach, S. M. F., Gupta, S., Hadzibabic, Z., Ketterle, W., 2003. Observation of bose-einstein condensation of molecules. *Phys. Rev. Lett.* 91, 250401.